

### 3 The Precambrian paleogeography of Laurentia

Nicholas L. Swanson-Hysell<sup>1</sup>

<sup>1</sup> Department of Earth and Planetary Science, University of California, Berkeley, CA 94720 USA

*This chapter is in preparation for the book Ancient Supercontinents and the Paleogeography of the Earth*

<sup>1</sup> **3.1 Introduction**

Laurentia was a major continent throughout the majority of the Proterozoic and is hypothesized to have had a central position in both the Paleoproterozoic Nuna and Neoproterozoic Rodinia supercontinents. The paleogeographic position of Laurentia is key to the development of reconstructions of Proterozoic paleogeography. There is a rich record of Precambrian paleomagnetic poles from Laurentia as well as an extensive geologic history of tectonism that are both key to evaluating and developing paleogeographic models. This chapter seeks to provide a concise review of these records.

<sup>9</sup> **3.2 Broad tectonic history overview**

Laurentia refers to the craton that forms the Precambrian core of North America (Fig. 1). Laurentia is comprised of multiple Archean provinces that had unique histories prior to their amalgamation in the Paleoproterozoic, as well as tectonic zones of crustal growth that post-date this assembly (Hoffman, 1989; Whitmeyer and Karlstrom, 2007). Collision between the Superior province and the composite Slave+Rae+Hearne provinces that resulted in the Trans-Hudson orogeny represents a major event in the formation of Laurentia (Corrigan et al., 2009). Terminal collision recorded in the Trans-Hudson orogen is estimated to have been ca. 1.86 to 1.82 Ga based on constraints such as U-Pb dating of monazite grains and zircon rims (Skipton et al., 2016; Weller and St-Onge, 2017, e.g.). A period of accretionary and collision orogenesis is recorded in the constituent provinces and terranes of Laurentia leading up to the terminal collision of the

20 Trans-Hudson orogeny. This overall story of rapid Paleoproterozoic amalgamation of Laurentia's  
21 constituent Archean provinces, including the terminal Trans-Hudson orogeny, was synthesized in  
22 the seminal *United Plates of America* paper of Hoffman (1988) and has been refined in the time  
23 since – particularly with additional geochronological constraints. Of most relevance here are the  
24 events that led to the suturing of more major Archean provinces: the Thelon orogen associated  
25 with the collision between the Slave and Rae provinces ca. 2.0 to 1.9 Ga (Hoffman, 1989); the  
26 Snowbird orogen associated with ca. 1.89 Ga collision between the Rae and Hearne provinces and  
27 associated terranes (Berman et al., 2007); the Nagssugtoqidian orogen due to the ca. 1.86 to 1.84  
28 Ga collision between the Rae and North Atlantic provinces (St-Onge et al., 2009); and the  
29 Torngat orogen resulting from the ca. 1.87 to 1.85 Ga collision of the Meta Incognita province  
30 (grouped with the Rae province in older compilations) with the North Atlantic province (St-Onge  
31 et al., 2009). As for the Wyoming province, many models posit that it was conjoined with Hearne  
32 and associated provinces at the time of the Trans-Hudson orogeny (e.g. St-Onge et al., 2009;  
33 Pehrsson et al., 2015) or was proximal to Hearne and Superior while still undergoing continued  
34 translation up to ca. 1.80 Ga (Whitmeyer and Karlstrom, 2007). A contrasting view has been  
35 proposed that the Wyoming province and Medicine Hat blocks was not conjoined with the  
36 other Laurentia provinces until ca. 1.72 Ga (Kilian et al., 2016). This interpretation is argued to  
37 be consistent with geochronological constraints on monazite and metamorphic zircon indicating  
38 active collisional orogenesis associated with the Big Sky orogen on the northern margin of the  
39 craton as late as ca. 1.75 to 1.72 Ga (Condit et al., 2015) and ca. 1.72 tectonomagmatic activity  
40 in the Black Hills region (Redden et al., 1990). However, the evidence for earlier orogenesis ca.  
41 1.78 to 1.75 in the Black Hills (Dahl et al., 1999; Hrncir et al., 2017), as well as high-grade  
42 tectonism as early as ca. 1.81 Ga in the Big Sky orogen (Condit et al., 2015), may support the  
43 interpretation of Hrncir et al. (2017) that ca. 1.72 Ga activity is a minor overprint on ca. 1.75  
44 terminal suturing between Wyoming and Superior. Regardless, in both of these interpretations,  
45 Wyoming is a later addition to Laurentia with final suturing post-dating ca. 1.82 Ga  
46 amalgamation of Archean provinces with the Trans-Hudson orogen further to the northeast.  
47 Overall, the collision of these Archean microcontinents between ca. 1.9 and 1.8 Ga lead to rapid  
48 amalgamation of the majority of the Laurentia craton.

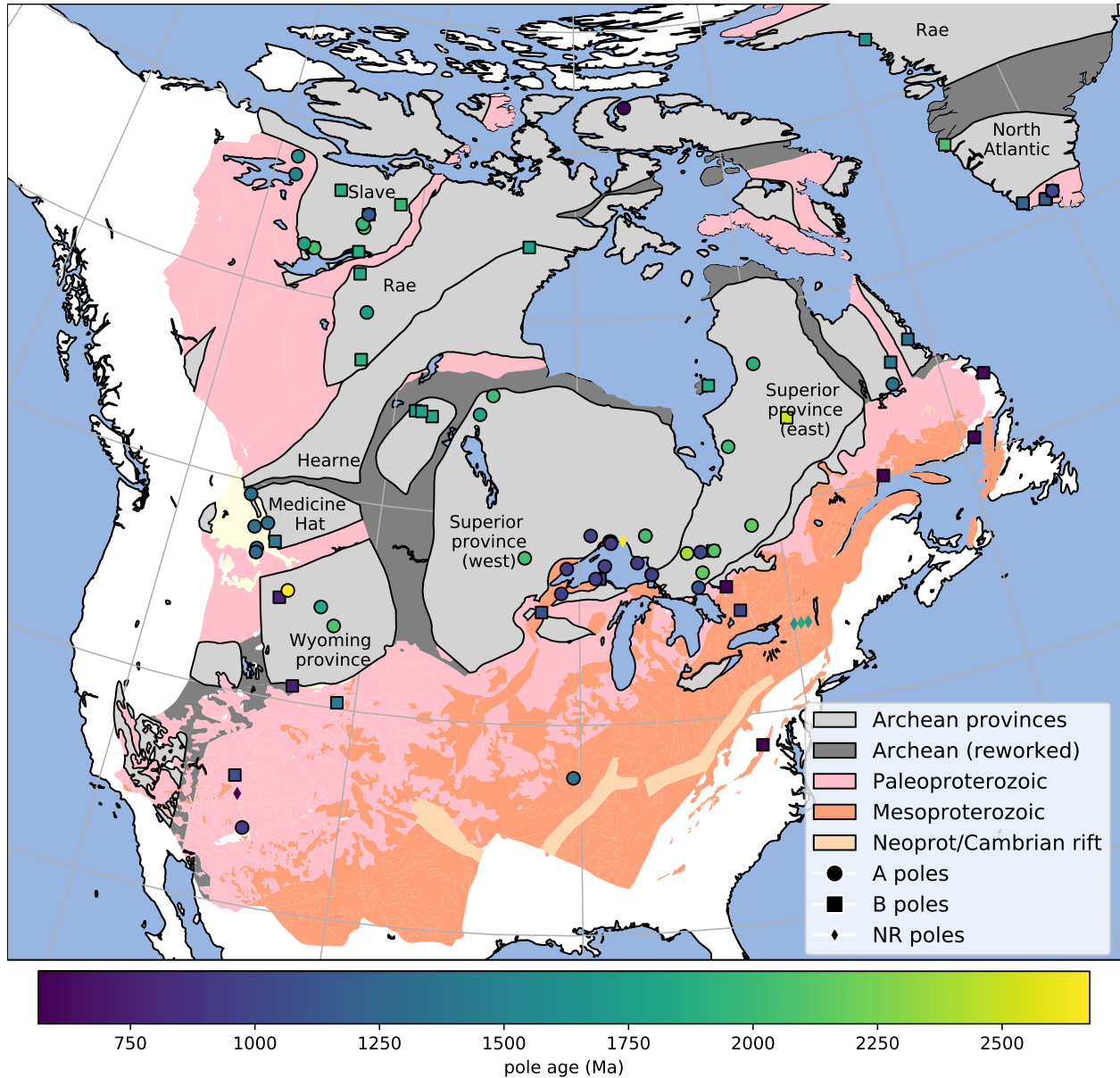


**Figure 1.** Simplified map of Laurentia showing the location of Archean provinces (labeled with text) and younger Paleoproterozoic and Mesoproterozoic crust (simplified from Whitmeyer and Karlstrom, 2007 with additions for Greenland based on St-Onge et al., 2009). The localities from which the compiled Precambrian paleomagnetic poles were developed are shown and colored by age. The circles (A rated poles) and squares (B rated poles) have been assessed by the Nordic workshop panel.

49 Crustal growth also progressed in the Paleoproterozoic through accretionary orogenesis. This  
50 accretion occurred within the Wopmay orogen through ca. 1.88 Ga arc-continent collision that led  
51 to the accretion of the Hottah terrane (the Calderian orogeny) and the subsequent emplacement  
52 of the Great Bear magmatic zone from ca. 1.88 to 1.84 Ga (Hildebrand et al., 2009). Coeval with  
53 the Trans-Hudson orogeny was the peripheral Penokean orogeny during which both microcontinent  
54 blocks (the Marshfield terrane) and arc terranes accreted on the southeastern margin of the west  
55 Superior province ca. 1.86 to 1.82 (Schulz and Cannon, 2007). Firm evidence of the end of the  
56 orogeny comes from the ca. 1.78 undeformed plutons of the post-Penokean East Central  
57 Minnesota Batholith (Holm et al., 2005).

58 In the paleogeographic model framework of Pehrsson et al. (2015), the collisions of provinces  
59 and terranes leading up to the Trans-Hudson orogeny mark the initial phase of assembly of the  
60 supercontinent Nuna. The Trans-Hudson orogeny itself is taken to be the terminal collision  
61 associated with the closure of the Manikewan Ocean that had previous been a large oceanic tract  
62 separating the Superior province from the composite Slave+Rae+Hearne+North Atlantic  
63 provinces (often referred to as the Churchill domain or plate; e.g. Skipton et al., 2016; Weller and  
64 St-Onge, 2017). The Pehrsson et al. (2015) model posits that this period terminal collision not  
65 only resulted in the amalgamation of Laurentia, but is also associated with the assembly of the  
66 supercontinent Nuna that is hypothesized to include other major Paleoproterozoic cratons  
67 including Siberia, Congo/São Francisco, West Africa, and Amazonia (Whitmeyer and Karlstrom,  
68 2007; Pehrsson et al., 2015).

69 Following the Trans-Hudson orogeny, the locus of orogenesis migrated to the exterior of  
70 Laurentia. This change marks a shift in the predominant style of Laurentia's growth as subsequent  
71 crustal growth occurred dominantly through accretion of juvenile crust along the southern and  
72 eastern margin of the nucleus of Archean provinces (Whitmeyer and Karlstrom, 2007; Figs. 1 and  
73 2). Determining the extent of these belts is complicated by poor exposure of them in the  
74 midcontinent relative to the exposure of the Archean provinces throughout the Canadian shield.  
75 Major growth of Laurentia following the amalgamation of these Archean provinces occurred  
76 associated with the arc-continent collision of the ca. 1.71 to 1.68 Ga Yavapai orogeny. Yavapai  
77 orogenesis is interpreted to have resulted from the accretion of a series of arc terranes that

78 collided with each other and Laurentia (Karlstrom et al., 2001). Yavapai accretion was followed  
79 by widespread emplacement of granitoid intrusions (Whitmeyer and Karlstrom, 2007). These  
80 intrusions are hypothesized to have stabilized the juvenile accreted terranes that subsequently  
81 remained part of Laurentia (Whitmeyer and Karlstrom, 2007). Subsequent accretionary  
82 orogenesis of the ca. 1.65–1.60 Ga Mazatzal Orogeny and associated plutonism lead to further  
83 crustal growth in the latest Paleoproterozoic (Karlstrom and Bowring, 1988). Laurentia's growth  
84 continued in the Mesoproterozoic along the southeast margin through further juvenile terrane and  
85 arc accretion. An interval of major plutonism occurred ca. 1.48–1.35 Ga leading to the formation  
86 of A-type granitoids throughout both Mesoproterozoic and Paleoproterozoic provinces extending  
87 from the southwest United States up to the Central Gneiss Belt of Ontario to the northeast of  
88 Georgian Bay (Slagstad et al., 2009). This plutonism is likely due to crustal melting within a  
89 back-arc region of ca. 1.50 to 1.43 Ga accretionary orogenesis (Bickford et al., 2015). Younger  
90 magmatic activity ca. 1.37 Ga of the Southern Granite–Rhyolite Province suggests a similar  
91 tectonic setting of accretionary orogenesis at that time (Bickford et al., 2015). While an active  
92 margin interpretation with magmatism in back-arc setting has gained traction within the  
93 literature with additional data, the tectonic setting is often described as enigmatic given earlier  
94 interpretations of an anorogenic setting (see references in Slagstad et al., 2009).

95 Accretionary orogenesis continued along the (south)east margin of Laurentia with the  
96 arc-continent collision of the ca. 1.25-1.22 Ga Elzevirian orogeny (McLelland et al., 2013). The  
97 subsequent ca. 1.19 to 1.16 Ga Shawinigan orogeny is interpreted to be due to the accretion of a  
98 terrane comprised of amalgamated arc volcanics and associated metasediments and is followed by  
99 a period of tectonic quiescence on the eastern margin of Laurentia until the collision orogenesis of  
100 the Grenvillian orogeny (McLelland et al., 2010). In the latest Mesoproterozoic (ca. 1.11-1.08  
101 Ga), a major intracontinental rift co-located with a large igneous province formed in Laurentia's  
102 interior leading to extension within the Archean Superior province and Paleoproterozoic  
103 provinces. This Midcontinent Rift lead to the formation of a thick succession of volcanics and  
104 mafic intrusions that are well-preserved in Laurentia's interior. Midcontinent Rift development  
105 ceased as major collisional orogenesis of the Grenvillian orogeny began (Swanson-Hysell et al.,  
106 2019). The Grenvillian orogeny was a protracted interval of continent-continent collision (ca. 1.09

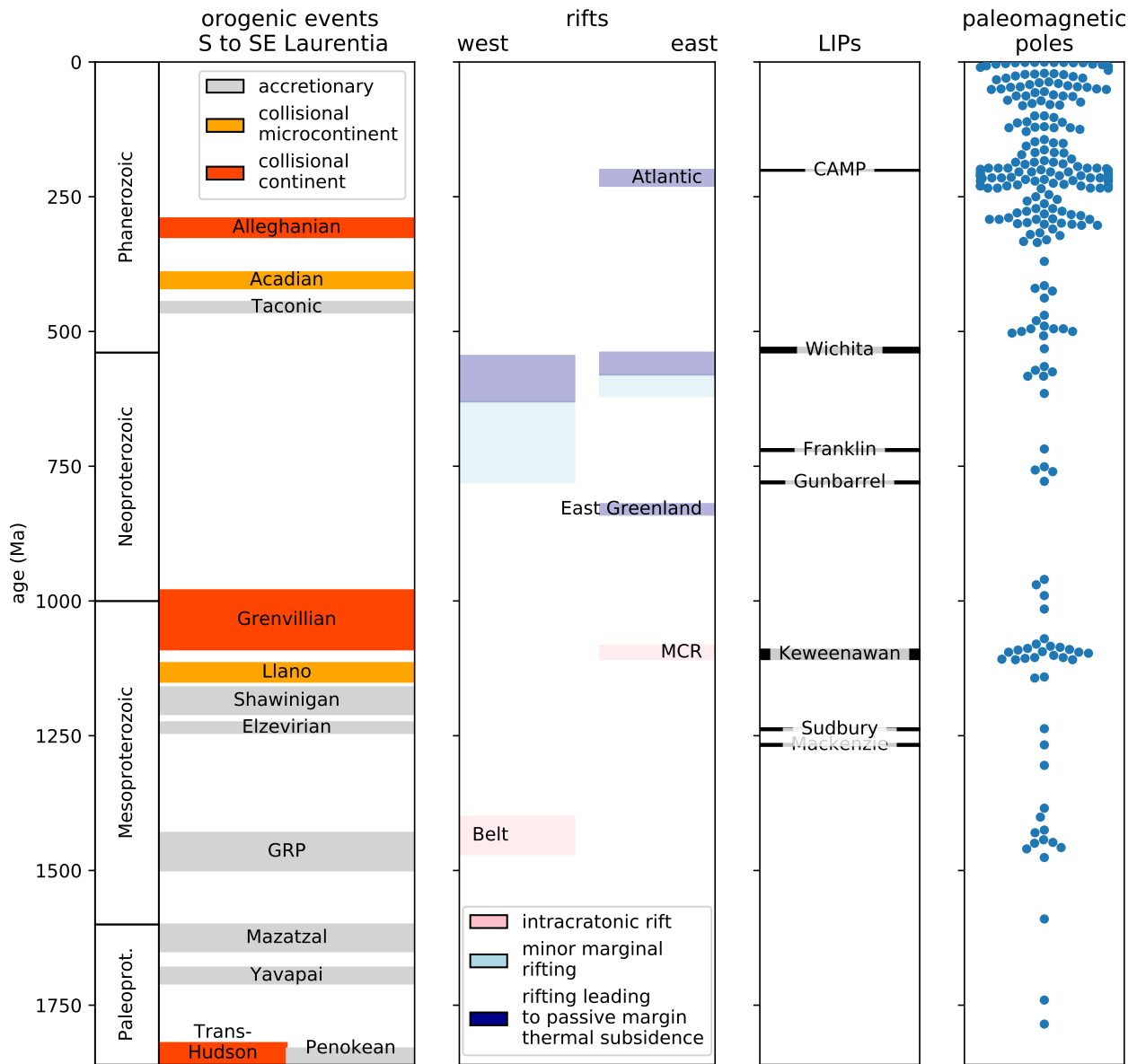


**Figure 2. Simplified timeline of Laurentia's tectonic history over the past ~1.8 billion years.** Brief summaries and references related to the orogenic and rifting episodes are given in the text. A timeline of large igneous provinces (LIPs) associated with typically brief and voluminous (or interpreted to be voluminous) volcanism is also shown. The interpreted age of paleomagnetic poles for Laurentia (not including separated terranes) compiled in this study for the Proterozoic and in Torsvik et al. (2012) for the Phanerozoic is shown.

<sup>107</sup> to 0.98 Ga) leading to amphibolite to granulite facies metamorphism through the orogen  
<sup>108</sup> (McLlland et al., 2010). The orogeny is interpreted to have resulted in the development of a  
<sup>109</sup> thick orogenic plateau (Rivers, 2008).

<sup>110</sup> There is significantly less preserved crustal growth on the western margin of Laurentia (Fig. 1)  
<sup>111</sup> and the Mesoproterozoic tectonic history is not as well elucidated as on the southern to eastern  
<sup>112</sup> margin. The 15 to 20 km thick package of sedimentary rocks of the Belt-Purcell Supergroup is  
<sup>113</sup> associated with a ca. 1.47 to 1.40 intracontinental rift – the tectonic setting of which is debated.  
<sup>114</sup> Hoffman (1989) proposed that it may be a remanent back-arc basin trapped within a continent,  
<sup>115</sup> while others envision it as being associated with continental rifting along the margin associated  
<sup>116</sup> with separation of a conjugate continent (Jones et al., 2015). This region is interpreted to have  
<sup>117</sup> been subsequently deformed during a ca. 1.36 to 1.33 event known as the East Kootenay orogeny  
<sup>118</sup> (McMechan and Price, 1982; Nesheim et al., 2012; McFarlane, 2015).

<sup>119</sup> This late Paleoproterozoic and Mesoproterozoic tectonic history provides significant  
<sup>120</sup> constraints on paleogeographic reconstructions. In particular, the long-lived history of  
<sup>121</sup> accretionary orogenesis along the southeast (present-day coordinates) of Laurentia from the  
<sup>122</sup> initiation of the Yavapai orogeny (ca. 1.71 Ga) to the end of the Shawinigan orogeny (ca. 1.06  
Ga) requires a long-lived open margin without a major conjugate continent up until the time of  
<sup>124</sup> terminal Grenvillian orogeny collision (Karlstrom et al., 2001). This constraint is incorporated  
<sup>125</sup> into models such as that of Zhang et al. (2012) and Pehrsson et al. (2015) which maintain a  
<sup>126</sup> long-lived convergent margin throughout the Mesoproterozoic, but in some reconstructions other  
<sup>127</sup> continental blocks are reconstructed into positions that are seemingly incompatible with this  
<sup>128</sup> record of accretionary orogenesis (e.g. Amazonia in Elming et al., 2009). The high-grade  
<sup>129</sup> metamorphism associated with the Ottawan phase of the Grenvillian orogeny itself requires a  
<sup>130</sup> collision between Laurentia and (an)other continent(s) ca. 1080 Ma – the geological observation  
<sup>131</sup> of which first lead to the formulation of the hypothesis of the supercontinent Rodinia (Hoffman,  
<sup>132</sup> 1991). Evidence of large-scale continent-continent collision at the time of the Ottawan Phase of  
<sup>133</sup> the Grenvillian orogeny is recorded in Texas, up through the Blue Ridge Appalachian inliers,  
<sup>134</sup> through Ontario and up to the Labrador Sea. This extensive and major collision orogenic history  
<sup>135</sup> recorded in Laurentia remains a strong piece of evidence that a supercontinent or

<sup>136</sup> (proto)supercontinent formed at the 1.0 Ga Mesoproterozoic to Neoproterozoic transition. The  
<sup>137</sup> term Grenville orogeny or Grenville belt is used rather loosely throughout much of the literature  
<sup>138</sup> to refer to any late Mesoproterozoic orogenic belt. The timeline of orogenesis on the Laurentia  
<sup>139</sup> margin has more nuanced constraints than this which can be comparatively assessed when  
<sup>140</sup> evaluating potential conjugate continents to Laurentia associated with the orogen (Fig. 2).

<sup>141</sup> The subsequent Neoproterozoic tectonic history of Laurentia is dominantly a record of rifting  
<sup>142</sup> (Fig. 2). Along the western margin of Laurentia, small-scale rifting occurred ca. 780 to 720 Ma  
<sup>143</sup> leading to deposition in basins that is recorded from the Death Valley region of SW Laurentia up  
<sup>144</sup> to the Mackenzie Mountains of NW Laurentia (Macdonald et al., 2012; Rooney et al., 2017).  
<sup>145</sup> However, this extensional basin development is relatively minor and predates the more significant  
<sup>146</sup> rifting that lead to passive margin thermal subsidence that did not occur until the Ediacaran  
<sup>147</sup> (closer to the ca. 539 Ma Neoproterozoic-Phanerozoic boundary; Bond et al., 1984; Levy and  
<sup>148</sup> Christie-Blick, 1991). The emplacement of the ca. 780 Ma Gunbarrel large igneous province along  
<sup>149</sup> this margin and the subsequent extension recorded in the basins is commonly interpreted to be  
<sup>150</sup> associated with the break-up of Laurentia and a conjugate continent to the western margin. If  
<sup>151</sup> this interpretation is correct, it is unclear why there would be minimal thermal subsidence until  
<sup>152</sup> the Ediacaran (post 635 Ma as in Levy and Christie-Blick, 1991 and Witkosky and Wernicke,  
<sup>153</sup> 2018). The geological evidence therefore supports active tectonism along the western margin of  
<sup>154</sup> Laurentia, but suggests that more dramatic lithospheric thinning occurred later than the timing  
<sup>155</sup> of rifting typically implemented in models of Rodinia break-up. One possibility, along the lines of  
<sup>156</sup> that proposed in Ross (1991), is that ca. 780 Ma extensional tectonism is an inboard record of  
<sup>157</sup> rifting and passive margin development that occurred further outboard. In this model,  
<sup>158</sup> subsequent continent rifting that drove lithospheric thinning, perhaps associated with the  
<sup>159</sup> departure of a microcontinent fragment rather than an already departed major conjugate  
<sup>160</sup> continent, would be the cause of Ediacaran to Cambrian thermal subsidence. The margin that  
<sup>161</sup> did experience large-scale rifting and associated passive margin thermal subsidence earlier in the  
<sup>162</sup> Neoproterozoic is the northeast Greenland margin (Fig. 2). Available geochronological  
<sup>163</sup> constraints and thermal subsidence modeling indicate ca. 820 Ma rifting followed by thermal  
<sup>164</sup> subsidence of a stable platform (Maloof et al., 2006; Halverson et al., 2018). These data suggest

165 that conjugate continental lithosphere rifted away from northeast Greenland ca. 820 Ma.

166 Extensive rifting that was followed by thermal subsidence occurred along the southeast to east  
167 Laurentia margin leading up to the Neoproterozoic-Phanerozoic boundary and is interpreted to be  
168 associated with the opening of the Iapetus ocean. A record of this rifting is preserved as rift  
169 basins that were part of failed arms (Rome trough, Reelfoot rift and Oklahoma aulacogen; Fig. 1)  
170 as well as prolonged Cambrian to Ordovician passive margin thermal subsidence along the margin  
171 (Bond et al., 1984; Whitmeyer and Karlstrom, 2007). The age of igneous intrusions that have  
172 been interpreted to be rift-related play a significant role in interpretations of this history such as  
173 in the rift development model of Burton and Southworth (2010). In this model,  
174 spatially-restricted rifting occurs ca. 760 to 680 Ma in the region of modern-day North Carolina  
175 and Virginia. Rifting ca. 620-580 Ma initiates in the region from modern-day New York to  
176 Newfoundland and by ca. 580 to 550 Ma rifting extends along the length of Laurentia's eastern  
177 margin. The last phases of this rifting appears to be associated with the separation of the  
178 Argentine pre-Cordillera Cuyania terrane (Dickerson and Keller, 1998). Cuyania is widely  
179 interpreted be a rifted fragment of SE Laurentia that separated associated with this early  
180 Cambrian rifting and subsequently became part of Gondwana when it collided with other terranes  
181 in the vicinity of the Rio de Plata craton during the Ordovician Famatinian orogeny (Martin  
182 et al., 2019). As with other rifts, it is difficult to distinguish the separation of a cratonic fragment  
183 as a microcontinent from the rifting of a major craton as the record that lingers on the craton is  
184 similar. One interpretation is that there was successful break-up along the eastern margin during  
185 the ca. 580 to 550 Ma interval of rifting prior to the ca. 539 Oklahoma aulacogen rifting that  
186 liberated the Cuyania microcontinent. The Maz-Arequipa-Rio Apa (MARA) block with which  
187 Cuyania collided (Martin et al., 2019) is likely a product of such rifting. Orogenesis between the  
188 MARA block and the Rio de Plata and Kalahari in the ca. 530 Ma Pampean orogeny (Casquet  
189 et al., 2018) predated the collision of Cuyania during the ca. 460 Famatinian orogeny in West  
190 Gondwana (Rapalini, 2018).

191 The eastern margin of Laurentia then went through the cycle of Appalachian orogenesis. As is  
192 visualized in Figure 2, there are parallels between the Grenville orogenic interval and the  
193 Appalachian orogenic interval in that there was a period of arc-continent collision (Shawinigan

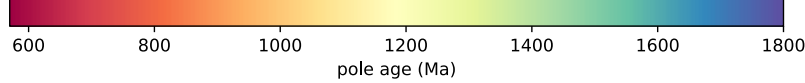
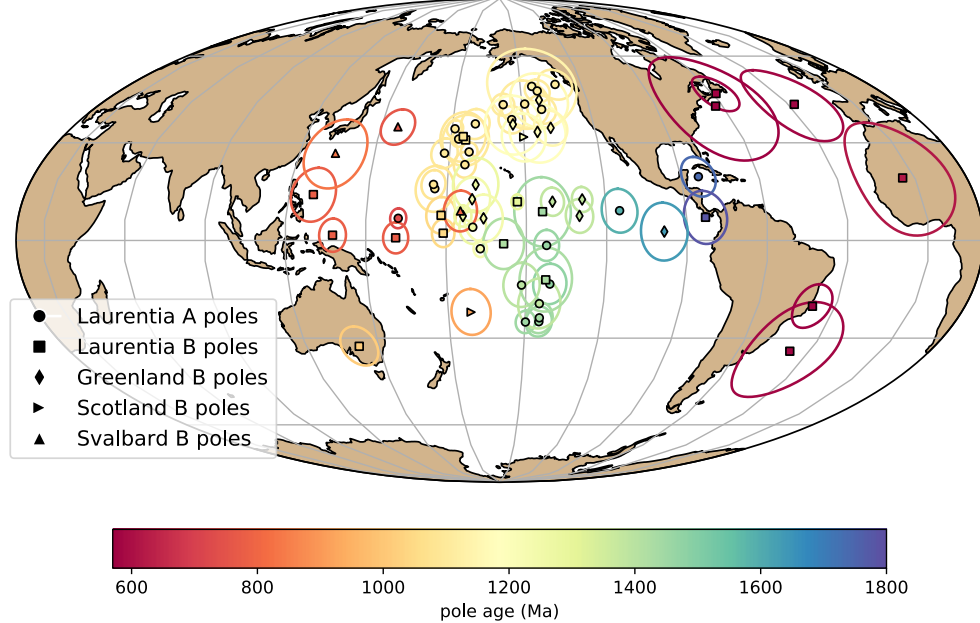
194 orogeny in the Grenville interval; Taconic orogeny in the Appalachian interval) followed by  
195 microcontinent accretion (Llano in the Grenville interval; Acadian in the Appalachian interval)  
196 that culminated in large-scale continent-continent collision (Grenvillian orogeny in the Grenville  
197 interval; Alleghanian in the Appalachian interval). These similarities are the consequence of an  
198 active margin facing an ocean basin that was progressively consumed until its consumption  
199 resulted in continent-continent collision. In the case of the Grenville interval, this terminal  
200 collision is interpreted to be associated with the assembly of the supercontinent Rodinia and in  
201 the Appalachian interval it is interpreted to be associated with the assembly of the supercontinent  
202 Pangea.

203 Even without considering other continents on Earth, the geological record of Paleoproterozoic  
204 collisional of Archean provinces combined with accretionary orogenesis at that time and through  
205 the rest of the Paleoproterozoic and Mesoproterozoic provides very strong evidence for mobile  
206 plate tectonics driving Laurentia's evolution throughout the past 2 billion years. This tectonic  
207 history inferred from geological data can be enhanced through integration with the paleomagnetic  
208 record.

### 209 **3.3 Paleomagnetic pole compilation**

210 In this chapter, I focus on the compilation of paleomagnetic poles developed through the Nordic  
211 Paleomagnetism Workshops with some additions and modifications (Fig. 3 and Table 2). The  
212 Nordic Paleomagnetism Workshops have taken the approach of using expert panels to assess  
213 paleomagnetic poles and assign them grades meant to convey the confidence that the community  
214 has in these results (Evans et al., this volume). While many factors associated with  
215 paleomagnetic poles can be assessed quantitatively through Fisher statistics and the precision of  
216 geochronological constraints, other aspects such as the degree to which available field tests  
217 constrain the magnetization to be primary require expert assessment. The categorizations used by  
218 the expert panel are 'A' and 'B' with the last panel meeting occurring in Fall 2017 in Leirubakki,  
219 Iceland. An 'A' rating refers to poles that are judged to be of such high-quality that they provide  
220 essential constraints that should be satisfied in paleogeographic reconstructions. A 'B' rating is  
221 associated with poles that are judged to likely provide a high-quality constraint, but have some

Poles for Laurentia (post-Paleoproterozoic amalgamation; with terranes)



Poles for Laurentia (pre-Paleoproterozoic amalgamation)

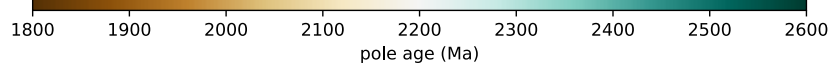
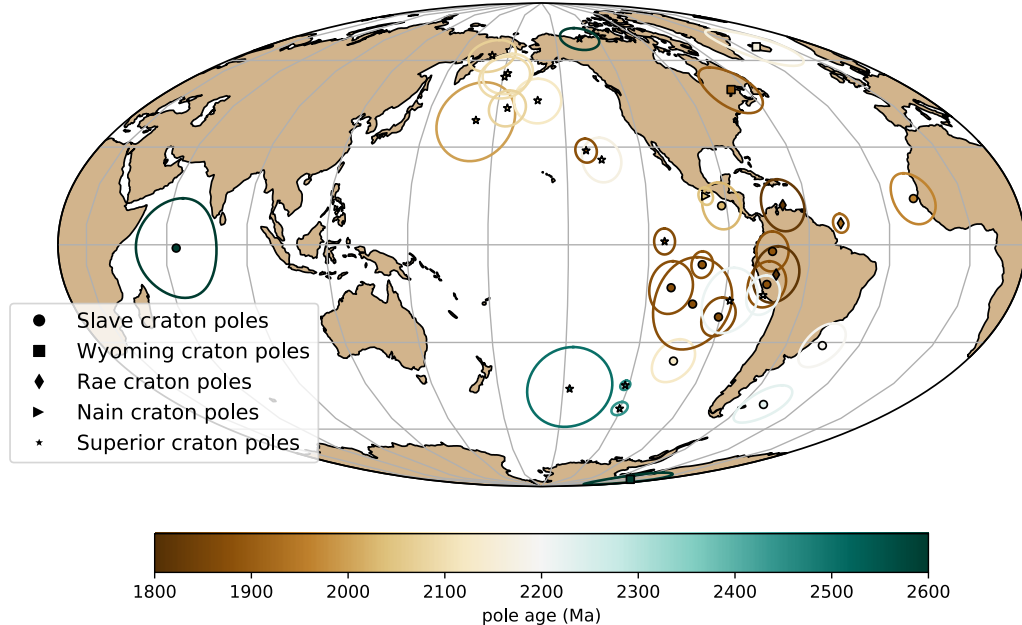


**Figure 3.** Top panel: Paleomagnetic poles from 1800 to 560 Ma for Laurentia (including Greenland, Scotland and Svalbard). Bottom panel: Paleomagnetic data for Archean Provinces prior to the amalgamation of Laurentia.

deficiency such as remaining ambiguity in the demonstration of primary remanence or the quality/precision of available geochronologic constraints. Additional poles that were not given an ‘A’ or ‘B’ classification at the Nordic Workshops are referred to as not-rated (‘NR’). These additional poles are taken from the Paleomagia database (Veikkolainen et al., 2014). Many of these poles are quite valuable for reconstruction and should not be dismissed from being considered in paleogeographic reconstructions. However, there are ambiguities associated with many of such poles not given Nordic ‘A’ or ‘B’ ratings in terms of how well the nature of the remanence is constrained including its age. For example, there are rich data associated with intrusive lithologies of the Grenville Province that are the available paleomagnetic constraints for Laurentia at the Mesoproterozoic-Neoproterozoic boundary. However, the ages of the remanence associated with these poles is complicated by the reality that the magnetization was acquired during exhumation and such cooling ages are more difficult to robustly constrain than the ages of remanence associated with dated eruptive units or shallow-level intrusions. As a result, the vast majority of Grenville Province poles are not given an ‘A’ or ‘B’ rating with the exception of the ‘B’ rated pole from the ca. 1015 Ma Haliburton intrusions. However, while any one of these Grenville poles could be interpreted to suffer from temporal uncertainty, the overall preponderance of poles in a similar location at the time suggests that they need to be taken seriously within any paleogeographic reconstruction of Laurentia (although note an alternative view of an allochthonous origin discussed below). In this compilation, the poles of Brown and McEnroe (2012) from the Adirondack highlands are used wherein the magnetic mineralogy and associated relative ages of remanence are well-constrained (Table 2). Additional not-rated poles included in the present compilation is the new pole for the ca. 1144 Ma Ontario lamprophyre dykes (Piispa et al., 2018) that strengthens the position of Laurentia at the time and coincides with the position of the poles from the ca. 1140 Ma Abitibi dikes (Ernst and Buchan, 1993). This pole will likely receive an ‘A’ rating when assessed at the next Nordic paleomagnetism workshop. Poles from the Chuar Group as presented in Eyster et al. (2019) are also included.

### <sup>248</sup> 3.4 Differential motion before Laurentia amalgamation

<sup>249</sup> Prior to the termination of the Trans-Hudson orogeny (before 1.8 Ga), paleomagnetic poles need  
<sup>250</sup> to be considered with respect to the individual Archean provinces. For the Superior province, an  
<sup>251</sup> additional complexity is that paleomagnetic poles from Siderian to Rhyacian Period (2.50 to 2.05  
<sup>252</sup> Ga) dike swarms, as well as deflection of dike trends, support an interpretation that there was  
<sup>253</sup> substantial Paleoproterozoic rotation of the western Superior province relative to the eastern  
<sup>254</sup> Superior province across the Kapuskasing Structural Zone (Bates and Halls, 1991; Evans and  
<sup>255</sup> Halls, 2010). This interpretation is consistent with the hypothesis of Hoffman (1988) that the  
<sup>256</sup> Kapuskasing Structural Zone represents major intracratonic uplift related to the Trans-Hudson  
<sup>257</sup> orogeny. Evans and Halls (2010) propose an Euler rotation of (51°N, 85°W, -14°CCW) to  
<sup>258</sup> reconstruct western Superior relative to eastern Superior and interpret that the rotation occurred  
<sup>259</sup> in the time interval of 2.07 to 1.87 Ga. I follow this interpretation and group the poles into  
<sup>260</sup> Superior (West) and Superior (East). Uncertainty remains with respect to whether the ca. 1.88  
<sup>261</sup> Ga Molson dikes pole pre-dates or post-dates this rotation and thus for the time being should be  
<sup>262</sup> considered solely in the western Superior province reference frame.

<sup>263</sup> There are poles in the compilation for the Slave, Wyoming, Rae, Superior and Nain provinces  
<sup>264</sup> prior to Laurentia amalgamation (Fig. 3 and Table 2). Overall, these data provide an  
<sup>265</sup> opportunity to re-evaluate the paleomagnetic evidence for relative motions between Archean  
<sup>266</sup> provinces prior to Laurentia assembly. A lingering question raised in Hoffman (1988) that still  
<sup>267</sup> remains is to what extent the Archean provinces each had independent drift histories with  
<sup>268</sup> significant separation or shared histories before experiencing fragmentation and reamalgamation.  
<sup>269</sup> The strongest analysis in this regard comes from comparisons between paleomagnetic poles  
<sup>270</sup> between the Superior and Slave provinces (Buchan et al., 2009; Mitchell et al., 2014; Buchan  
<sup>271</sup> et al., 2016). High-quality paleomagnetic poles from these two provinces provide strong support  
<sup>272</sup> for differential motion between the Superior and Slave provinces between 2.2 and 1.8 Ga with the  
<sup>273</sup> two provinces not being in their relative orientation to one another either and having distinct pole  
<sup>274</sup> paths as constrained by 5 time periods of nearly coeval poles from 2.23 and 1.89 Ga (Fig. 4;  
<sup>275</sup> Buchan et al., 2016. These data provide paleomagnetic support for the Superior and Slave  
<sup>276</sup> provinces having independent histories of differential motion. They also support the hypothesis

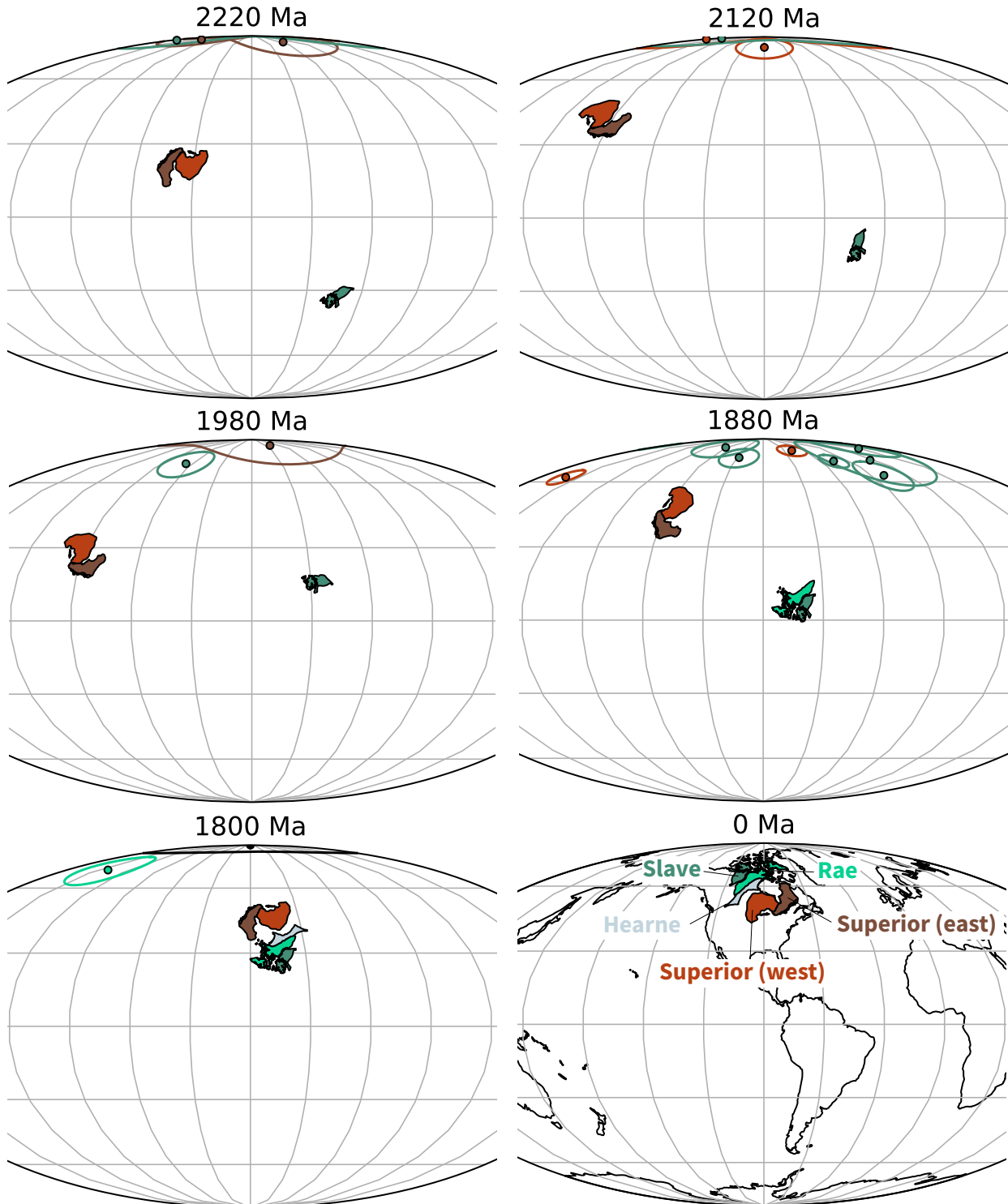


**Figure 4.** Paleogeographic reconstructions developed using poles from the Superior, Slave and Rae provinces. Paleomagnetic poles are shown colored to match their respective province with these provinces shown in present-day coordinates and labeled in the 0 Ma panel. Poles with ages that are within 25 million years of the given time slice are shown. The relatively well-resolved pole paths from the Superior and Slave provinces (Fig. 3) that are utilized for these reconstructions provide strong support for differential plate tectonic motion between 2220 and 1850 Ma.

277 that the Trans-Hudson orogeny is the result of terminal collision associated with the closure of an  
278 ocean basin between the Superior province and the Hearne+Rae+Slave provinces.

279 Reconstructions developed for this chapter of the Superior and Slave provinces using these poles  
280 are shown in Figure 4 and illustrate the difference in implied orientation and paleolatitude that  
281 results from these well-constrained poles.

### 282 **3.5 Paleogeography of an assembled Laurentia**

283 Following the amalgamation of the Archean provinces in Laurentia ca. 1.8 Ga, poles from each  
284 part of Laurentia can be considered to reflect the position of the entire composite craton. It is  
285 worth considering the possibility that poles from zones of Paleoproterozoic and Mesoproterozoic  
286 accretion could be allochthonous to the craton. Halls (2015) argued that this was the case for late  
287 Mesoproterozoic and early Neoproterozoic poles from east of the Grenvillian allochthon boundary  
288 fault. However, the majority of researchers have considered these poles to post-date major  
289 differential motion and be associated with cooling during collapse of a thick orogenic plateau  
290 developed during continent-continent collision (e.g. Brown and McEnroe, 2012). Poles with a  
291 B-rating are also included in the composite that come from Greenland, Svalbard and Scotland.

292 These terranes were once part of contiguous Laurentia, but have subsequently rifted away. These  
293 poles need to be rotated into the Laurentia reference frame prior to use for tectonic  
294 reconstruction and I apply the rotations shown in Table 1. The Euler pole and rotation is quite  
295 well-constrained for Greenland as it is associated with recent opening of Baffin Bay and the  
296 Labrador Sea (for which the rotation of Roest and Srivastava, 1989 is used). The reconstruction  
297 of Scotland is associated with the opening of the Atlantic (for which the rotation employed by  
298 Torsvik and Cocks, 2017 is used) which is well-constrained but has more uncertainty associated  
299 with the Euler pole than that for Greenland. The reconstruction of Svalbard is more challenging  
300 given a multi-state tectonic history involving both translation within the Caledonides and  
301 subsequent rifting. The preferred Euler of Maloof et al. (2006) is used here that designed, in  
302 particular, to honor the high degree of similarity between Tonian sediments in East Greenland  
303 (Hoffman et al., 2012) and those of East Svalbard (Maloof et al., 2006).

304 Through the Proterozoic, there are intervals where there are abundant paleomagnetic poles

305 that constrain Laurentia's position and intervals when the record is quite sparse (shown colored  
306 by age in Fig. 3). To further visualize the temporal coverage of the poles and to summarize the  
307 motion, implied paleolatitudes for an interior point on Laurentia are shown in Figure 5. The ages  
308 of poles are also shown in comparison to the simplified summary of tectonic events in Figure 2.  
309 Both collisional and extensional tectonism can result in the formation of lithologies that can be  
310 used to develop paleomagnetic poles either as a result of basin formation, magmatism or both. In  
311 addition, intraplate magmatism resulting from plume-related large-igneous provinces can lead to  
312 paleomagnetic poles in periods that are otherwise characterized by tectonic quiescence (e.g. the  
313 ca. 1267 Ma Mackenzie LIP; Fig. 2). Intracontinental rifts have led to the highest density of poles  
314 both in the case of the ca. 1.4 Ga Belt Supergroup and the ca. 1.1 Ga Midcontinent Rift (Fig. 2).  
315 The quality and resolution of the record from the Midcontinent Rift is aided by the voluminous  
316 magmatism that occurred in conjunction with basin formations that enables the development of  
317 well-calibrated apparent polar wander path (Swanson-Hysell et al., 2019). The late Tonian Period  
318 also has a number of poles including the Gunbarrel LIP (ca. 780 Ma) and Franklin LIP (ca. 720  
319 Ma), as well as similarly-aged sedimentary rocks from western Laurentia basins (Eyster et al.,  
320 2019). Overall, the record of paleomagnetic poles has a lot of internal consistency in intervals for  
321 which there is high-resolution coverage. These data result in the progressive paths agreement  
322 between poles such as ascending up to the Logan Loop, down the Keweenawan Track  
323 (Swanson-Hysell et al., 2019) to the Grenville Loop prior to a temporal gap before the late Tonian  
324 (ca. 775 to 720 Ma) path (Eyster et al., 2019).

325 Data from other terranes add resolution to the record. In particular, data from Greenland  
326 adds 12 poles between 1385 and 1160 Ma when there are only 4 poles from mainland Laurentia.  
327 Given that the rotation between Greenland and mainland Laurentia is well-constrained (Table 1),  
328 once rotated these poles can be used for reconstruction of the entire continent. The reliability of  
329 this approach gains credence through the good agreement between the ca. 1633 Ma Melville Bugt  
330 diabase dykes pole from Greenland (Halls et al., 2011) and the ca. 1590 Ma Western Channel  
331 diabase pole of mainland Laurentia (Irving and Park, 1972). Similarly, there is good agreement  
332 between the ca. 1267 Ma Mackenzie dykes pole of Laurentia (Buchan et al., 2000) and coeval  
333 poles from Greenland such as the ca. 1275 Ma North Qoroq intrusives (Piper, 1992) and Kungnat

<sup>334</sup> Ring dyke (Piper, 1977). Furthermore, the Greenland poles with ages that fall between the ca.  
<sup>335</sup> 1237 Ma Sudbury dikes and ca. 1143 Ma lamprophyre dykes pole of mainland Laurentia are  
<sup>336</sup> consistent with constraints on either side from the mainland while filling in the ascending limb of  
<sup>337</sup> the path leading up to the apex of 1140 to 1108 Ma poles known as the Logan Loop (Fig. ??).

<sup>338</sup> An exception to this overall agreement between poles from Greenland and mainland Laurentia  
<sup>339</sup> occurs ca. 1382 Ma. There are poles of this age from Greenland associated with the Zig-Zag Dal  
<sup>340</sup> basalts and related intrusions (Marcussen and Abrahamsen, 1983; Abrahamsen and Van Der Voo,  
<sup>341</sup> 1987). However, these poles are in a distinct location from poles of similar age associated with the  
<sup>342</sup> Belt Supergroup (e.g. the McNamara Formation and Pilcher/Garnet Range and Libby  
<sup>343</sup> Formations; Elston et al., 2002). Additionally, the older Belt Supergroup poles form a more  
<sup>344</sup> southerly population than time-equivalent poles from elsewhere in Laurentia such as the Mistastin  
<sup>345</sup> Pluton. There are potential complications associated with the Belt Supergroup being exposed  
<sup>346</sup> within thrust sheets with significant Cenozoic Mesozoic and Cenozoic deformation. However,  
<sup>347</sup> vertical axis rotations of the Belt region are not able to bring the Belt poles into agreement with  
<sup>348</sup> those from Laurentia or Greenland nor is translation away from the craton. Another potential  
<sup>349</sup> complication is that the remanence used for the development of the Belt Supergroup resides in  
<sup>350</sup> hematite. As a result, there is the potential for inclination-flattening within the sedimentary rocks  
<sup>351</sup> from which poles are developed. However, applying a moderate inclination factor of  $f = 0.6$  also  
<sup>352</sup> does not bring the poles into congruence with the Zig-Zag basalts. There is the potential that the  
<sup>353</sup> hematite could be the result of post-depositional oxidation (the remanence of the Purcell lavas  
<sup>354</sup> pole is also held by hematite) however the overall coherency of the pole directions and the  
<sup>355</sup> presence of reversals has been taken as evidence that the remanence is primary (Elston et al.,  
<sup>356</sup> 2002). At present, it is unclear which poles are a better representation of Laurentia's position ca.  
<sup>357</sup> 1400 Ma.

<sup>358</sup> Another challenging portion of the Laurentia record is that for the Ediacaran Period where  
<sup>359</sup> there is little consistency between poles of similar age (Figs. 3 and ??). As a result, there are  
<sup>360</sup> poles that imply both low-latitude and high-latitude positions of Laurentia between 615 and 565  
<sup>361</sup> Ma. One explanation for these variable pole positions is that they are the result of large-scale  
<sup>362</sup> oscillatory true polar wander in the Ediacaran that has influenced poles in Baltica and West

363 Africa as well (McCausland et al., 2007; Robert et al., 2017). Another possibility is that the lack  
364 of congruency between poles in this point in the record is due to a particularly weak and  
365 non-dipolar geomagnetic field (Abrajevitch and Van der Voo, 2010; Bono et al., 2019). Regardless  
366 of mechanism, the Ediacaran data stand out as anomalous relative to the coherency of the rest of  
367 the poles in the composite (Fig. 5).

368 Synthesizing the compilation of paleomagnetic poles for Laurentia into a composite path over  
369 the past 1.8 billion years presents a challenge given the highly variable temporal coverage. The  
370 method typically applied in the Phanerozoic is to develop synthesized pole paths either through  
371 fitting spherical splines through the data or calculating binned running means where the Fisher  
372 mean of poles within a given interval are calculated (Torsvik et al., 2012). Applying such an  
373 approach can reduce the effect of spurious poles in regions of high data density where seeking to  
374 satisfy every mean pole position would result in jerky motion.

375 A synthesized pole path for Laurentia is developed here and used to develop a continuous  
376 paleogeographic reconstruction of Laurentia constrained by the compilation of paleomagnetic  
377 poles. The paleolatitude implied by this continuous model is shown in Figure 5. This path is  
378 based on Laurentia data alone which means that it is poorly constrained through intervals of  
379 sparse data (950-850 Ma for example). One could use interpretations of paleogeographic  
380 connections with other cratons (e.g. Baltica in the early Neoproterozoic) to fill in such portions of  
381 the path, however the result then becomes model-dependent without being constrained by data  
382 from Laurentia itself. In portions of the record with a more dense record of poles, such as ca.  
383 1450, a calculated running mean is used to integrate constraints from multiple poles. This  
384 method follows the approach taken in the Phanerozoic (e.g. Torsvik et al., 2012 wherein all poles  
385 within a 20 Myr interval are averaged with the interval than progressively moved forward in 10  
386 Myr steps. When there are isolated ‘A’ grade poles without other temporally-similar poles, these  
387 poles are fully satisfied in model. Where there are no constraints a simple interpolation between  
388 constraints is made. While data from Scotland and Svalbard are associated with Laurentia, the  
389 Scotland poles are poorly constrained in time and the Svalbard rotation to Laurentia is uncertain.  
390 These poles are not utilized in the simple Laurentia model which means that the model as shown  
391 does not include oscillatory true polar wander interpreted to have occurred ca. 810 and 790 Ma

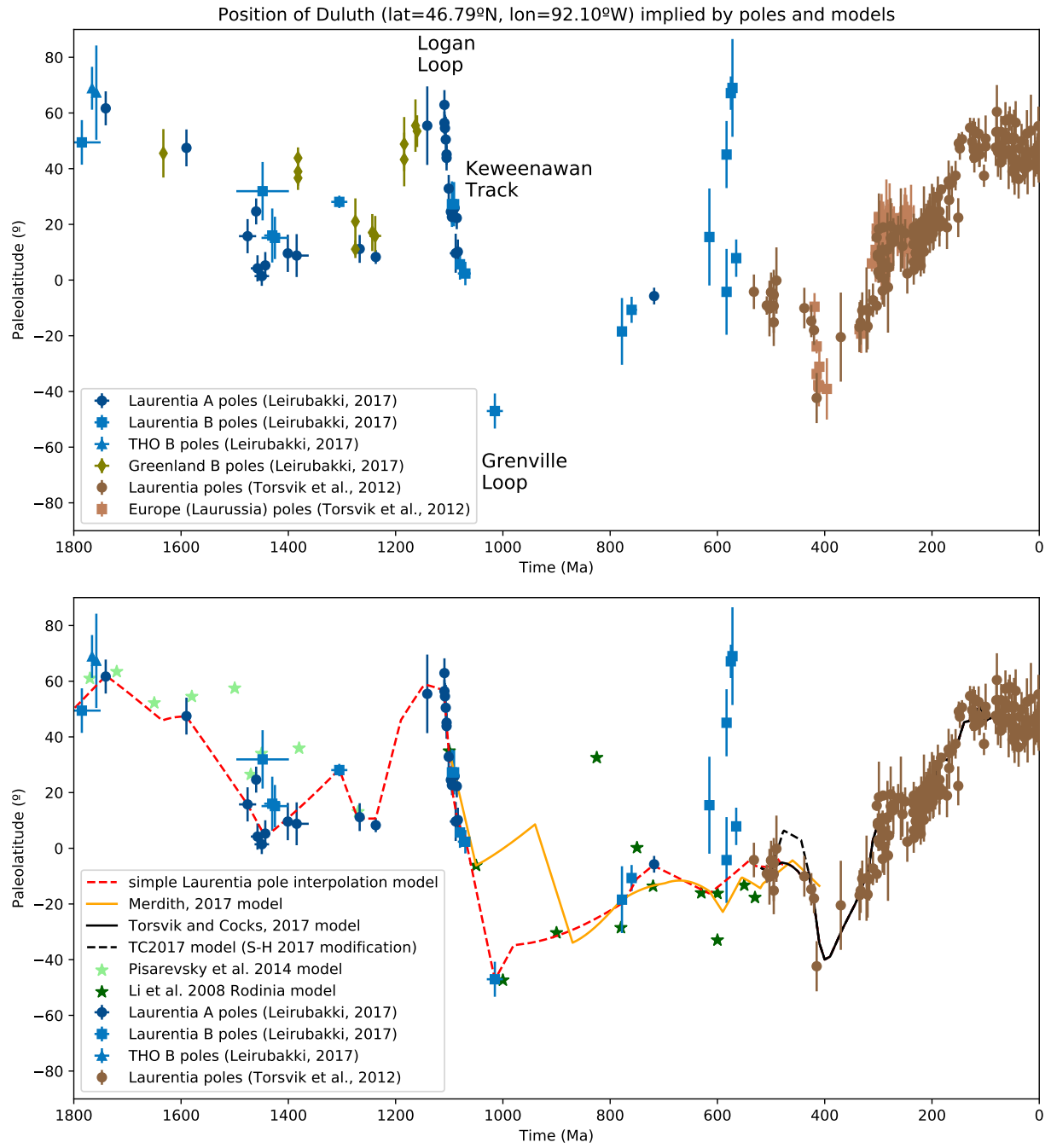


**Figure 5. Top panel:** Paleolatitude implied by paleomagnetic poles from Laurentia and associated blocks for Duluth (lat=46.79°N, lon=92.10°W). The paleomagnetic poles are compiled in Table 2. **Bottom panel:** Paleolatitude implied by Laurentia poles compared with that implied by published paleogeographic models and the simple Laurentia model used in this chapter for the reconstructions in Figure 7.

<sup>392</sup> based on data from Svalbard (Maloof et al., 2006).

<sup>393</sup> One downside of a running mean approach is that it pulls the mean to regions of high data  
<sup>394</sup> density. As was shown in Swanson-Hysell et al. (2019), this behavior can reduce motion along an  
<sup>395</sup> apparent polar wander path. As a result, for the portion of the reconstruction during the interval  
<sup>396</sup> of time ca. 1110 to 1070 Ma, I utilize an Euler pole inversion from Swanson-Hysell et al. (2019).

<sup>397</sup> Paleogeographic snapshots for the past position of Laurentia reconstructed using this synthesis  
<sup>398</sup> of the paleomagnetic poles are shown in Figure 7. These reconstructions use the tectonic elements  
<sup>399</sup> as defined by Whitmeyer and Karlstrom (2007) with these elements being progressively added  
<sup>400</sup> associated with Laurentia's accretionary growth. As a reminder to the reader, paleomagnetic  
<sup>401</sup> poles provide constraints on the paleolatitude of a continental block as well as its orientation  
<sup>402</sup> (which way was north relative to the block). While they provide constraints in this regard, they  
<sup>403</sup> do not provide constraints in and of themselves to the longitudinal position of the block. Other  
<sup>404</sup> approaches to obtain paleolongitude utilize geophysical hypotheses such as assuming that large  
<sup>405</sup> low shear velocity provinces have been stable plume-generating zones in the lower mantle to  
<sup>406</sup> which plumes can be reconstructed (Torsvik et al., 2014) or that significant pole motion in certain  
<sup>407</sup> time intervals is associated with true polar wander axes that switch through time in conjunction  
<sup>408</sup> with the supercontinent cycle (Mitchell et al., 2012). In Figure 7, Laurentia is centered on the  
<sup>409</sup> longitudinal position of Duluth with the orientation and paleolatitude being constrained by the  
<sup>410</sup> paleomagnetic pole compilation as synthesized in the simple Laurentia pole interpolation model.

### <sup>411</sup> 3.6 Comparing paleogeographic models to the paleomagnetic compilation

<sup>412</sup> Seeking to develop comprehensive global continuous paleogeographic models is a major  
<sup>413</sup> challenge given the need to integrate and satisfy diverse geological and paleomagnetic data types.  
<sup>414</sup> Continually improving constraints related to tectonic setting from improved geologic and  
<sup>415</sup> geochronologic data need to be carefully integrated with the database of paleomagnetic poles.  
<sup>416</sup> Paleomagnetic poles compilations themselves are evolving with better data and improved  
<sup>417</sup> geochronology. Efforts such as this volume are therefore essential to present the state-of-the-art in  
<sup>418</sup> terms of existing constraints that can be used to evaluate current models and set the stage for

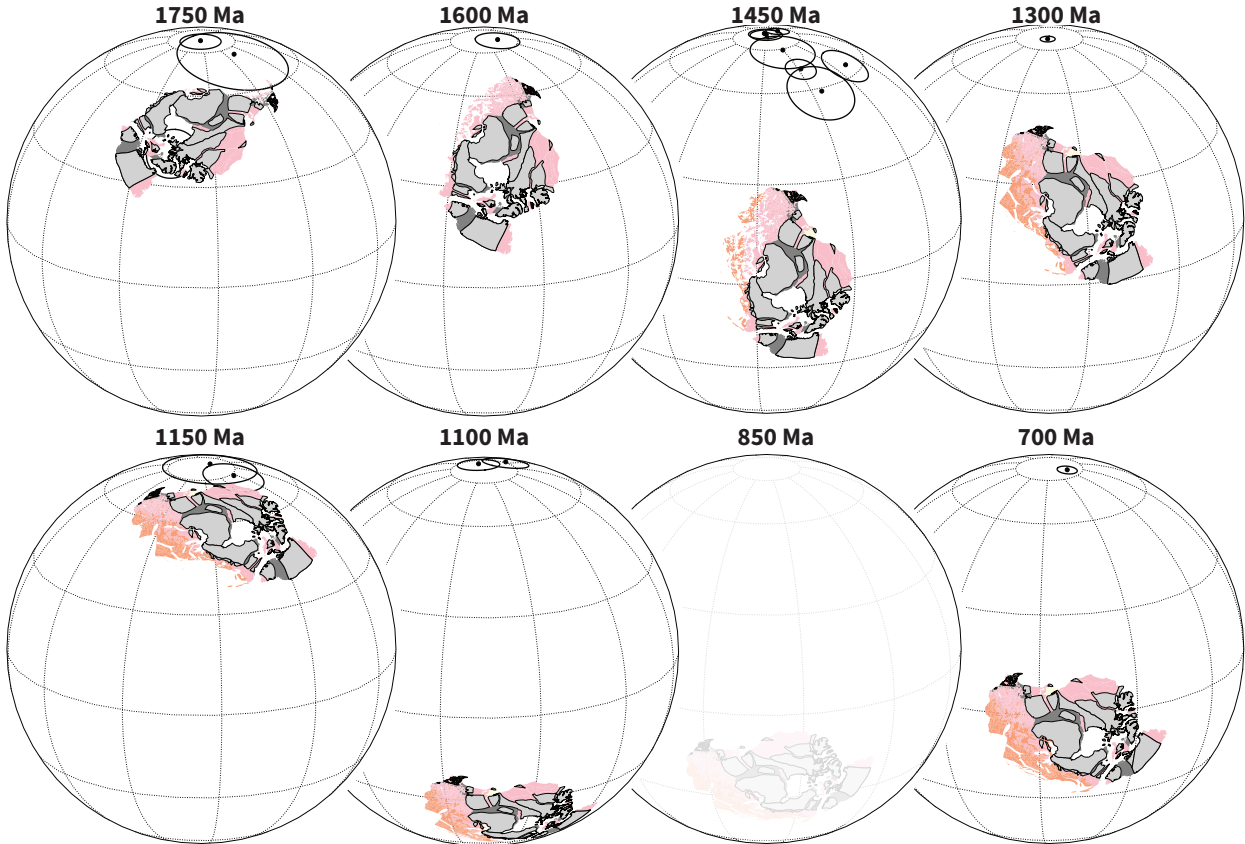


**Figure 6.** Paleogeographic reconstructions of Laurentia at time intervals through the Proterozoic that are well-constrained by paleomagnetic data. These reconstructions use the simple Laurentia pole interpolation model that is shown in Figure 5 and use this model to reconstruct the tectonic elements of Whitmeyer and Karlstrom (2007) shown in Figure 1. Modern coastlines are maintained in these polygons so that the rotated orientations can be interpreted by the reader in comparison to Figure 1.

419 future progress.

420 There is an overall lack of published continuous models in the literature for the Proterozoic  
 421 that can be compared to the compilation of paleomagnetic poles presented herein. The approach  
 422 in the community for many years has been to publish models as snapshots at given time intervals  
 423 presented in figures without publishing continuous rotation parameters. With the further  
 424 adoption of software tools such as GPlates, there has been significant progress in the publication  
 425 of continuous paleogeographic models constrained by paleomagnetic poles through the  
 426 Phanerozoic (540 Ma to present; e.g. Torsvik et al., 2012).

427 An exception to the paucity of published continuous paleogeographic models for the  
 428 Precambrian is the Neoproterozoic model of Merdith et al. (2017) which is shown in comparison

429 to the constraints for Laurentia in Figure 5. The extent to which the implied position of  
430 Laurentia in Merdith et al. (2017) is consistent with the compiled paleomagnetic constraints can  
431 be visualized in Figure 5. As noted above, the development of such models is challenging and the  
432 researchers need to balance varying constraints. The focus here will be on the extent to which  
433 this model satisfies the available paleomagnetic poles for Laurentia. The model does not honor  
434 the Grenville loop (e.g. go to moderately high southerly latitudes ca. 1000 Ma) which is a striking  
435 departure from the paleomagnetic record and standard paleogeographic models. Additionally, the  
436 implemented plate motion strays from the younger poles of the Keweenawan Track and does not  
437 honor the Franklin LIP pole Denyszyn et al. (2009b) despite its ‘A’ Nordic rating. The Franklin  
438 pole is taken to be a key constraint at the Tonian/Cryogenian boundary that provides evidence of  
439 the supercontinent Rodinia being equatorial and for the Sturtian glaciation having extended to  
440 equatorial latitudes.

441 There are more published models that show snapshots and publish rotation parameters  
442 associated with given time intervals such as the Rodinia model of Li et al. (2008) and the  
443 Mesoproterozoic model of Pisarevsky et al. (2014), but did not publish parameters for a  
444 continuous model. The position for Laurentia implied by the Euler poles given for the model  
445 snapshots of these studies are shown in Figure 5.

### 446 3.7 Conclusion

447 There is strong evidence both in the geological and paleomagnetic record of Laurentia for  
448 differential plate tectonic motion between 2.2 and 1.8 Ga. The continued history of accretionary  
449 orogenesis and the evaluation of Laurentia’s pole path in comparison to other continents from 1.8  
450 Ga onward supports the continual operation of plate tectonics throughout the rest of the  
451 Proterozoic and Phanerozoic as well. While this evidence fits with the majority of interpretations  
452 of the timing of initiation of modern-style plate tectonics (see summary in Korenaga, 2013), there  
453 continue to be arguments proposing that a stagnant lid persisted through the Mesoproterozoic  
454 Era (1.6 to 1.0 Ga) and into the Neoproterozoic with plate tectonics not initiating until ca. 0.8  
455 Ga (Hamilton, 2011; Stern and Miller, 2018). These arguments rest largely on the relative lack of  
456 the types of low-temperature high-pressure metamorphic rocks such as blueschists that form in

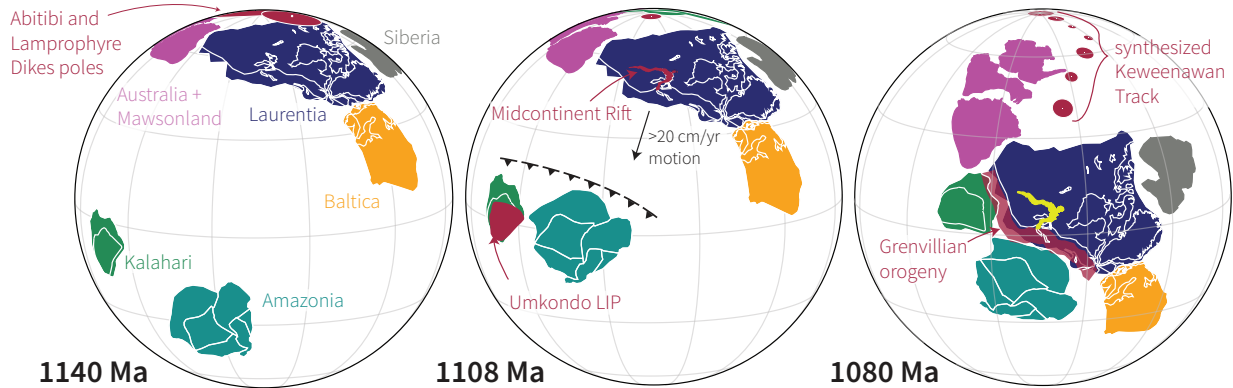


**Figure 7.** Paleogeographic reconstructions of Laurentia and other select Proterozoic continents leading up to Rodinia assembly in the late Mesoproterozoic modified from Swanson-Hysell et al. (2019). The record of paleomagnetic poles implies rapid motion which is consistent with the timing of collisional orogenesis associated with the Grenvillian orogeny.

457 subduction zones in the Proterozoic relative to the Phanerozoic (Stern et al., 2013). An  
 458 alternative interpretation for this lack of blueschists in the Proterozoic is that such a shift in  
 459 metamorphic regime is the predicted result of secular evolution of mantle chemistry rather than a  
 460 harbinger of the onset of plate tectonics (Palin and White, 2015). While this line of evidence is  
 461 intriguing, to argue that there was not differential plate tectonic motion in the Paleoproterozoic  
 462 and Mesoproterozoic is to ignore a vast breadth and depth of geological and paleomagnetic data.

463 As an example, consider the record of Laurentia in the late Mesoproterozoic. As can be seen in  
 464 Table 2, there is a fantastic quantity of high-quality paleomagnetic poles between 1110 and 1070  
 465 Ma. These poles constrain rapid motion of Laurentia along

466 The paleogeographic record of Laurentia is rich in constraints through the Precambrian both  
 467 in terms of the geological and geochronological constraints on tectonism and the record of  
 468 paleomagnetic poles. As can be seen in the Chapters on Archean paleogeography (Salminen et al.,  
 469 this volume), Nuna (Elming et al., this volume) and Rodinia (Evans et al., this volume), these  
 470 constraints are at the center of developing paleogeographic models through the Precambrian and  
 471 will continue to be moving forward.

472 **Acknowledgements**

473 Many participants in the Nordic Paleomagnetism Workshop have contributed to the compilation  
474 and evaluation of the pole list utilized herein. Particular acknowledgement goes to David Evans  
475 for maintaining and distributing the compiled pole lists as well as additional efforts of Lauri  
476 Pesonen in maintaining the Paleomagia database (Veikkolainen et al., 2014). GPlates, and in  
477 particular the pyGPlates API, was utilized in this work (Müller et al., 2018). Figures were made  
478 using Matplotlib (Hunter, 2007) in conjunction with cartopy (Met Office, 2010 - 2015) and  
479 pmagpy (Tauxe et al., 2016) within an interactive Python environment (Pérez and Granger,  
480 2007). This work was supported by NSF CAREER Grant EAR-1847277 awarded to N.L.S.-H.  
481 The code, data, and reconstructions used in this paper are openly available in this repository:  
482 [https://github.com/Swanson-Hysell-Group/Laurentia\\_Paleogeography](https://github.com/Swanson-Hysell-Group/Laurentia_Paleogeography).

483 **References**

- 484 Abrahamsen, N. and Van Der Voo, R., 1987, Palaeomagnetism of middle Proterozoic (c. 1.25 Ga) dykes from central  
485 North Greenland: Geophysical Journal International, v. 91, p. 597–611, doi:10.1111/j.1365-246x.1987.tb01660.x.
- 486 Abrajevitch, A. and Van der Voo, R., 2010, Incompatible Ediacaran paleomagnetic directions suggest an equatorial  
487 geomagnetic dipole hypothesis: Earth and Planetary Science Letters, v. 293, p. 164–170.
- 488 Bates, M. P. and Halls, H. C., 1991, Broad-scale Proterozoic deformation of the central Superior Province revealed  
489 by paleomagnetism of the 2.45 Ga Matachewan dyke swarm: Canadian Journal of Earth Sciences, v. 28, p.  
490 1780–1796, doi:10.1139/e91-159.
- 491 Berman, R., Davis, A., and Pehrsson, S., 2007, Collisional Snowbird tectonic zone resurrected: Growth of Laurentia  
492 during the 1.9 Ga accretionary phase of the Hudsonian orogeny: Geology, v. 35, p. 911–914,  
493 doi:10.1130/G23771A.1.
- 494 Bickford, M., Van Schmus, W., Karlstrom, K., Mueller, P., and Kamenov, G., 2015,  
495 Mesoproterozoic-trans-Laurentian magmatism: A synthesis of continent-wide age distributions, new SIMS U-Pb  
496 ages, zircon saturation temperatures, and Hf and Nd isotopic compositions: Precambrian Research, v. 265, p.  
497 286–312, doi:10.1016/j.precamres.2014.11.024.
- 498 Bond, G., Nickleson, P., and Kominz, M., 1984, Breakup of a supercontinent between 625 and 555 Ma: new  
499 evidence and implications for continental histories: Earth and Planetary Science Letters, v. 70, p. 325–345,  
500 doi:10.1016/0012-821X(84)90017-7.

- 501 Bono, R. K., Tarduno, J. A., Nimmo, F., and Cottrell, R. D., 2019, Young inner core inferred from Ediacaran  
502 ultra-low geomagnetic field intensity: *Nature Geoscience*, v. 12, p. 143–147, doi:10.1038/s41561-018-0288-0.
- 503 Books, K., 1972, Paleomagnetism of some Lake Superior Keweenawan rocks: U.S. Geological Survey Professional  
504 Paper, v. P 0760, p. 42.
- 505 Borradaile, G. and Middleton, R., 2006, Proterozoic paleomagnetism in the Nipigon Embayment of northern  
506 Ontario: Pillar Lake Lava, Wawieg Troctolite and Gunflint Formation tuffs: *Precambrian Research*, v. 144, p.  
507 69–91, doi:10.1016/j.precamres.2005.10.007.
- 508 Brown, L. L. and McEnroe, S. A., 2012, Paleomagnetism and magnetic mineralogy of Grenville metamorphic and  
509 igneous rocks, Adirondack Highlands, USA: *Precambrian Research*, v. 212–213, p. 57–74,  
510 doi:10.1016/j.precamres.2012.04.012.
- 511 Buchan, K., Mertanen, S., Park, R., Pesonen, L., Elming, S. A., Abrahamsen, N., and Bylund, G., 2000, Comparing  
512 the drift of Laurentia and Baltica in the Proterozoic: the importance of key paleomagnetic poles:  
513 *Tectonophysics*, v. 319, p. 167–198.
- 514 Buchan, K. L., LeCheminant, A. N., and van Breemen, O., 2009, Paleomagnetism and U–Pb geochronology of the  
515 Lac de Gras diabase dyke swarm, Slave Province, Canada: implications for relative drift of Slave and Superior  
516 provinces in the Paleoproterozoic: *Canadian Journal of Earth Sciences*, v. 46, p. 361–379, doi:10.1139/e09-026.
- 517 Buchan, K. L., LeCheminant, A. N., and van Breemen, O., 2012, Malley diabase dykes of the Slave craton,  
518 Canadian Shield: U–Pb age, paleomagnetism, and implications for continental reconstructions in the early  
519 Paleoproterozoic: *Canadian Journal of Earth Sciences*, v. 49, p. 435–454, doi:10.1139/e11-061.
- 520 Buchan, K. L., Mitchell, R. N., Bleeker, W., Hamilton, M. A., and LeCheminant, A. N., 2016, Paleomagnetism of  
521 ca. 2.13–2.11 Ga Indin and ca. 1.885 Ga Ghost dyke swarms of the Slave craton: Implications for the Slave  
522 craton APW path and relative drift of Slave, Superior and Siberian cratons in the Paleoproterozoic: *Precambrian  
523 Research*, v. 275, p. 151–175, doi:10.1016/j.precamres.2016.01.012.
- 524 Buchan, K. L., Mortensen, J. K., and Card, K. D., 1993, Northeast-trending early Proterozoic dykes of southern  
525 Superior Province: multiple episodes of emplacement recognized from integrated paleomagnetism and U–Pb  
526 geochronology: *Canadian Journal of Earth Sciences*, v. 30, p. 1286–1296, doi:10.1139/e93-110.
- 527 Burton, W. C. and Southworth, S., 2010, A model for Iapetan rifting of Laurentia based on Neoproterozoic dikes  
528 and related rocks: From Rodinia to Pangea: The Lithotectonic Record of the Appalachian Region, p. 455–476,  
529 doi:10.1130/2010.1206(20).
- 530 Casquet, C., Dahlquist, J. A., Verdecchia, S. O., Baldo, E. G., Galindo, C., Rapela, C. W., Pankhurst, R. J.,  
531 Morales, M. M., Murra, J. A., and Mark Fanning, C., 2018, Review of the Cambrian Pampean orogeny of

- 532 Argentina; a displaced orogen formerly attached to the Saldania Belt of South Africa?: Earth-Science Reviews, v.  
533 177, p. 209–225, doi:10.1016/j.earscirev.2017.11.013.
- 534 Condit, C. B., Mahan, K. H., Ault, A. K., and Flowers, R. M., 2015, Foreland-directed propagation of high-grade  
535 tectonism in the deep roots of a Paleoproterozoic collisional orogen, SW Montana, USA: *Lithosphere*, p. L460.1,  
536 doi:10.1130/l460.1.
- 537 Corrigan, D., Pehrsson, S., Wodicka, N., and de Kemp, E., 2009, The Palaeoproterozoic Trans-Hudson Orogen: a  
538 prototype of modern accretionary processes: Geological Society, London, Special Publications, v. 327, p. 457–479,  
539 doi:10.1144/sp327.19.
- 540 Dahl, P. S., Holm, D. K., Gardner, E. T., Hubacher, F. A., and Foland, K. A., 1999, New constraints on the timing  
541 of Early Proterozoic tectonism in the Black Hills (South Dakota), with implications for docking of the Wyoming  
542 province with Laurentia: *Geological Society of America Bulletin*, v. 111, p. 1335–1349,  
543 doi:10.1130/0016-7606(1999)111<1335:ncotto>2.3.co;2.
- 544 Denyszyn, S. W., Davis, D. W., and Halls, H. C., 2009a, Paleomagnetism and U–Pb geochronology of the Clarence  
545 Head dykes, Arctic Canada: orthogonal emplacement of mafic dykes in a large igneous province: *Canadian*  
546 *Journal of Earth Sciences*, v. 46, p. 155–167, doi:10.1139/E09-011.
- 547 Denyszyn, S. W., Halls, H. C., Davis, D. W., and Evans, D. A. D., 2009b, Paleomagnetism and U–Pb geochronology  
548 of Franklin dykes in High Arctic Canada and Greenland: a revised age and paleomagnetic pole constraining block  
549 rotations in the Nares Strait region: *Canadian Journal of Earth Sciences*, v. 46, p. 689–705, doi:10.1139/E09-042.
- 550 Dickerson, P. W. and Keller, M., 1998, The Argentine Precordillera: its odyssey from the Laurentian Ouachita  
551 margin towards the Sierras Pampeanas of Gondwana: Geological Society, London, Special Publications, v. 142,  
552 p. 85–105, doi:10.1144/gsl.sp.1998.142.01.05.
- 553 Donadini, F., Pesonen, L. J., Korhonen, K., Deutsch, A., and Harlan, S. S., 2011, Paleomagnetism and  
554 paleointensity of the 1.1 Ga old diabase sheets from central Arizona: *Geophysica*, v. 47, p. 3–30.
- 555 Elming, S. Å., D’Agrella-Filho, M. S., Page, L. M., Tohver, E., Trindade, R. I. F., Pacca, I. I. G., Geraldes, M. C.,  
556 and Teixeira, W., 2009, A palaeomagnetic and  $^{40}\text{Ar}/^{39}\text{Ar}$  study of late precambrian sills in the SW part of the  
557 Amazonian craton: Amazonia in the Rodinia reconstruction: *Geophysical Journal International*, v. 178, p.  
558 106–122.
- 559 Elston, D. P., Enkin, R. J., Baker, J., and Kisilevsky, D. K., 2002, Tightening the Belt: Paleomagnetic-stratigraphic  
560 constraints on deposition, correlation, and deformation of the Middle Proterozoic (ca. 1.4 Ga) Belt-Purcell  
561 Supergroup, United States and Canada: *GSA Bulletin*, v. 114, p. 619–638,  
562 doi:10.1130/0016-7606(2002)114<619:TTBPSC>2.0.CO;2.

- 563 Emslie, R. F., Irving, E., and Park, J. K., 1976, Further paleomagnetic results from the Michikamau Intrusion,  
564 Labrador: Canadian Journal of Earth Sciences, v. 13, p. 1052–1057, doi:10.1139/e76-108.
- 565 Ernst, R. and Buchan, K., 1993, Paleomagnetism of the Abitibi dike swarm, southern Superior Province, and  
566 implications for the Logan Loop: Canadian Journal of Earth Science, v. 30, p. 1886–1897, doi:10.1139/e93-167.
- 567 Evans, D. and Halls, H., 2010, Restoring Proterozoic deformation within the Superior craton: Precambrian  
568 Research, v. 183, p. 474 – 489, doi:10.1016/j.precamres.2010.02.007.
- 569 Evans, M. E. and Bingham, D. K., 1973, Paleomagnetism of the Precambrian Martin Formation, Saskatchewan:  
570 Canadian Journal of Earth Sciences, v. 10, p. 1485–1493, doi:10.1139/e73-141.
- 571 Evans, M. E. and Hoye, G. S., 1981, Paleomagnetic results from the lower proterozoic rocks of Great Slave Lake and  
572 Bathurst Inlet areas, Northwest Territories: *In* Proterozoic Basins of Canada; Geological Survey of Canada,  
573 Paper 81-10, Natural Resources Canada/ESS/Scientific and Technical Publishing Services, doi:10.4095/109374.
- 574 Eyster, A., Weiss, B. P., Karlstrom, K., and Macdonald, F. A., 2019, Paleomagnetism of the Chuar Group and  
575 evaluation of the late Tonian Laurentian apparent polar wander path with implications for the makeup and  
576 breakup of Rodinia: GSA Bulletin, doi:10.1130/b32012.1.
- 577 Fahrig, W. and Bridgwater, D., 1976, Late Archean-early Proterozoic paleomagnetic pole positions from west  
578 Greenland: *In* Windley, B., ed., Early History of the Earth, Wiley, p. 427–442.
- 579 Fahrig, W. F. and Jones, D. L., 1976, The paleomagnetism of the Helikian Mistastin pluton, Labrador, Canada:  
580 Canadian Journal of Earth Sciences, v. 13, p. 832–837, doi:10.1139/e76-086.
- 581 Fairchild, L. M., Swanson-Hysell, N. L., Ramezani, J., Sprain, C. J., and Bowring, S. A., 2017, The end of  
582 Midcontinent Rift magmatism and the paleogeography of Laurentia: Lithosphere, v. 9, p. 117–133,  
583 doi:10.1130/L580.1.
- 584 Gala, M. G., Symons, D. T. A., and Palmer, H. C., 1995, Paleomagnetism of the Jan Lake Granite, Trans-Hudson  
585 Orogen: Saskatchewan Geological Survey Summary of Investigations, v. 95-4.
- 586 Halls, H., 1974, A paleomagnetic reversal in the Osler Volcanic Group, northern Lake Superior: Canadian Journal  
587 of Earth Science, v. 11, p. 1200–1207, doi:10.1139/e74-113.
- 588 Halls, H. C., 2015, Paleomagnetic evidence for ~4000 km of crustal shortening across the 1 Ga Grenville orogen of  
589 North America: Geology, v. 43, p. 1051–1054, doi:10.1130/G37188.1.
- 590 Halls, H. C., Davis, D. W., Stott, G. M., Ernst, R. E., and Hamilton, M. A., 2008, The Paleoproterozoic Marathon  
591 Large Igneous Province: New evidence for a 2.1 Ga long-lived mantle plume event along the southern margin of  
592 the North American Superior Province: Precambrian Research, v. 162, p. 327–353,  
593 doi:10.1016/j.precamres.2007.10.009.

- 594 Halls, H. C., Hamilton, M. A., and Denyszyn, S. W., 2011, The Melville Bugt Dyke Swarm of Greenland: A  
595 Connection to the 1.5-1.6 Ga Fennoscandian Rapakivi Granite Province?, Springer Berlin Heidelberg, p. 509–535:  
596 doi:10.1007/978-3-642-12496-9{\\_}27.
- 597 Halls, H. C. and Hanes, J. A., 1999, Paleomagnetism, anisotropy of magnetic susceptibility, and argon–argon  
598 geochronology of the Clearwater anorthosite, Saskatchewan, Canada: Tectonophysics, v. 312, p. 235–248,  
599 doi:10.1016/s0040-1951(99)00166-3.
- 600 Halverson, G. P., Porter, S. M., and Gibson, T. M., 2018, Dating the late Proterozoic stratigraphic record:  
601 Emerging Topics in Life Sciences, v. 2, p. 137–147, doi:10.1042/etls20170167.
- 602 Hamilton, W. B., 2011, Plate tectonics began in Neoproterozoic time, and plumes from deep mantle have never  
603 operated: Lithos, v. 123, p. 1–20, doi:10.1016/j.lithos.2010.12.007.
- 604 Harlan, S., 1993, Paleomagnetism of Middle Proterozoic diabase sheets from central Arizona: Canadian Journal of  
605 Earth Science, v. 30, p. 1415–1426.
- 606 Harlan, S., Geissman, J., and Snee, L., 1997, Paleomagnetic and  $^{40}\text{Ar}/^{39}\text{Ar}$  geochronologic data from late  
607 Proterozoic mafic dykes and sills, Montana and Wyoming: USGS Professional Paper, v. 1580, p. 16.
- 608 Harlan, S. S. and Geissman, J. W., 1998, Paleomagnetism of the middle Proterozoic Electra Lake Gabbro, Needle  
609 Mountains, southwestern Colorado: Journal of Geophysical Research: Solid Earth, v. 103, p. 15,497–15,507,  
610 doi:10.1029/98jb01350.
- 611 Harlan, S. S., Geissman, J. W., and Snee, L. W., 2008, Paleomagnetism of Proterozoic mafic dikes from the Tobacco  
612 Root Mountains, southwest Montana: Precambrian Research, v. 163, p. 239–264.
- 613 Harlan, S. S., Snee, L. W., Geissman, J. W., and Brearley, A. J., 1994, Paleomagnetism of the middle proterozoic  
614 laramie anorthosite complex and sherman granite, southern laramie range, wyoming and colorado: Journal of  
615 Geophysical Research: Solid Earth, v. 99, p. 17,997–18,020, doi:10.1029/94jb00580.
- 616 Henry, S., Mauk, F., and Van der Voo, R., 1977, Paleomagnetism of the upper Keweenawan sediments: Nonesuch  
617 Shale and Freda Sandstone: Canadian Journal of Earth Science, v. 14, p. 1128–1138, doi:10.1139/e77-103.
- 618 Hildebrand, R. S., Hoffman, P. F., and Bowring, S. A., 2009, The Calderian orogeny in Wopmay orogen (1.9 Ga),  
619 northwestern Canadian Shield: Geological Society of America Bulletin, v. 122, p. 794–814, doi:10.1130/B26521.1.
- 620 Hnat, J. S., van der Pluijm, B. A., and Van der Voo, R., 2006, Primary curvature in the Mid-Continent Rift:  
621 Paleomagnetism of the Portage Lake Volcanics (northern Michigan, USA): Tectonophysics, v. 425, p. 71–82,  
622 doi:10.1016/j.tecto.2006.07.006.
- 623 Hoffman, P., 1991, Did the breakout of Laurentia turn Gondwana inside out?: Science, v. 252, p. 1409–1412.

- 624 Hoffman, P. F., 1988, United plates of America, the birth of a craton: Early Proterozoic assembly and growth of  
625 Laurentia: *Annual Review of Earth and Planetary Sciences*, v. 16, p. 543–603,  
626 doi:10.1146/annurev.ea.16.050188.002551.
- 627 Hoffman, P. F., 1989, Speculations on Laurentia's first gigayear (2.0 to 1.0 Ga): *Geology*, v. 17, p. 135–138,  
628 doi:10.1130/0091-7613(1989)017<0135:SOLSGF>2.3.CO;2.
- 629 Hoffman, P. F., Halverson, G. P., Domack, E. W., Maloof, A. C., Swanson-Hysell, N. L., and Cox, G. M., 2012,  
630 Cryogenian glaciations on the southern tropical paleomargin of Laurentia (NE Svalbard and East Greenland),  
631 and a primary origin for the upper Russøya (Islay) carbon isotope excursion: *Precambrian Research*, v. 206–207,  
632 p. 137–158, doi:10.1016/j.precamres.2012.02.018.
- 633 Holm, D. K., Van Schmus, W. R., MacNeill, L. C., Boerboom, T. J., Schweitzer, D., and Schneider, D., 2005, U-Pb  
634 zircon geochronology of Paleoproterozoic plutons from the northern midcontinent, USA: Evidence for subduction  
635 flip and continued convergence after geon 18 Penokean orogenesis: *Geological Society of America Bulletin*, v. 117,  
636 p. 259, doi:10.1130/b25395.1.
- 637 Hrncir, J., Karlstrom, K., and Dahl, P., 2017, Wyoming on the run—Toward final Paleoproterozoic assembly of  
638 Laurentia: COMMENT: *Geology*, v. 45, p. e411–e411, doi:10.1130/g38826c.1.
- 639 Hunter, J. D., 2007, Matplotlib: A 2D graphics environment: *Computing in Science & Engineering*, v. 9, p. 90–95,  
640 doi:10.1109/MCSE.2007.55.
- 641 Irving, E., 2004, Early Proterozoic geomagnetic field in western Laurentia: implications for paleolatitudes, local  
642 rotations and stratigraphy: *Precambrian Research*, v. 129, p. 251–270, doi:10.1016/j.precamres.2003.10.002.
- 643 Irving, E. and McGlynn, J. C., 1979, Palaeomagnetism in the Coronation Geosyncline and arrangement of  
644 continents in the middle Proterozoic: *Geophysical Journal International*, v. 58, p. 309–336,  
645 doi:10.1111/j.1365-246X.1979.tb01027.x.
- 646 Irving, E. and Park, J. K., 1972, Hairpins and superintervals: *Canadian Journal of Earth Sciences*, v. 9, p.  
647 1318–1324, doi:10.1139/e72-115.
- 648 Jones, J. V., Daniel, C. G., and Doe, M. F., 2015, Tectonic and sedimentary linkages between the Belt-Purcell basin  
649 and southwestern Laurentia during the Mesoproterozoic, ca. 1.60–1.40 Ga: *Lithosphere*, v. 7, p. 465–472,  
650 doi:10.1130/l438.1.
- 651 Karlstrom, K. E., Ahall, K.-I., Harlan, S. S., Williams, M. L., McLellan, J., and Geissman, J. W., 2001, Long-lived  
652 (1.8–1.0 Ga) convergent orogen in southern Laurentia, its extensions to Australia and Baltica, and implications  
653 for refining Rodinia: *Precambrian Research*, v. 111, p. 5–30, doi:10.1016/S0301-9268(01)00154-1.
- 654 Karlstrom, K. E. and Bowring, S. A., 1988, Early Proterozoic assembly of tectonostratigraphic terranes in  
655 southwestern North America: *The Journal of Geology*, v. 96, p. 561–576, doi:10.1086/629252.

- 656 Kean, W., Williams, I., and Feeney, J., 1997, Magnetism of the Keweenawan age Chengwatana lava flows, northwest  
657 Wisconsin: Geophysical Research Letters, v. 24, p. 1523–1526, doi:10.1029/97gl00993.
- 658 Kilian, T. M., Bleeker, W., Chamberlain, K., Evans, D. A. D., and Cousens, B., 2015, Palaeomagnetism,  
659 geochronology and geochemistry of the Palaeoproterozoic Rabbit Creek and Powder River dyke swarms:  
660 implications for Wyoming in supercraton Superia: Geological Society, London, Special Publications, v. 424, p.  
661 15–45, doi:10.1144/sp424.7.
- 662 Kilian, T. M., Chamberlain, K. R., Evans, D. A., Bleeker, W., and Cousens, B. L., 2016, Wyoming on the  
663 run—Toward final Paleoproterozoic assembly of Laurentia: Geology, v. 44, p. 863–866, doi:10.1130/g38042.1.
- 664 Korenaga, J., 2013, Initiation and evolution of plate tectonics on earth: Theories and observations: Annual Review  
665 of Earth and Planetary Sciences, v. 41, p. 117–151, doi:10.1146/annurev-earth-050212-124208.
- 666 Kulakov, E. V., Smirnov, A. V., and Diehl, J. F., 2013, Paleomagnetism of ~1.09 Ga Lake Shore Traps (Keweenaw  
667 Peninsula, Michigan): new results and implications: Canadian Journal of Earth Sciences, v. 50, p. 1085–1096,  
668 doi:10.1139/cjes-2013-0003.
- 669 Levy, M. and Christie-Blick, N., Nicholas, 1991, Tectonic subsidence of the early Paleozoic passive continental  
670 margin in eastern California and southern Nevada: Geological Society of America Bulletin, v. 103, p. 1590–1606,  
671 doi:10.1130/0016-7606(1991)103<1590:tsotep>2.3.co;2.
- 672 Li, Z. X. et al., 2008, Assembly, configuration, and break-up history of Rodinia: A synthesis: Precambrian  
673 Research, v. 160, p. 179–210, doi:10.1016/j.precamres.2007.04.021.
- 674 Macdonald, F., Halverson, G., Strauss, J., Smith, E., Cox, G., Sperling, E., and Roots, C., 2012, Early  
675 Neoproterozoic basin formation in Yukon, Canada: Implications for the make-up and break-up of Rodinia:  
676 Geoscience Canada, v. 39.
- 677 Maloof, A., Halverson, G., Kirschvink, J., Schrag, D., Weiss, B., and Hoffman, P., 2006, Combined paleomagnetic,  
678 isotopic and stratigraphic evidence for true polar wander from the Neoproterozoic Akademikerbreen Group,  
679 Svalbard, Norway: Geological Society of America Bulletin, v. 118, p. 1099–1124, doi:10.1130/B25892.1.
- 680 Marcussen, C. and Abrahamsen, N., 1983, Palaeomagnetism of the Proterozoic Zig-Zag Dal Basalt and the  
681 Midsommerso Dolerites, eastern North Greenland: Geophysical Journal International, v. 73, p. 367–387,  
682 doi:10.1111/j.1365-246x.1983.tb03321.x.
- 683 Martin, E. L., Collins, W. J., and Spencer, C. J., 2019, Laurentian origin of the Cuyania suspect terrane, western  
684 Argentina, confirmed by Hf isotopes in zircon: GSA Bulletin, doi:10.1130/b35150.1.
- 685 McCausland, P. J. A., Hankard, F., Van der Voo, R., and Hall, C. M., 2011, Ediacaran paleogeography of  
686 Laurentia: Paleomagnetism and 40Ar-39Ar geochronology of the 583 Ma Baie des Moutons syenite, Quebec:  
687 Precambrian Research, v. 187, p. 58–78, doi:10.1016/j.precamres.2011.02.004.

- 688 McCausland, P. J. A., Van der Voo, R., and Hall, C. M., 2007, Circum-Iapetus paleogeography of the  
689 Precambrian–Cambrian transition with a new paleomagnetic constraint from Laurentia: Precambrian Research,  
690 v. 156, p. 125–152, doi:10.1016/j.precamres.2007.03.004.
- 691 McFarlane, C. R., 2015, A geochronological framework for sedimentation and Mesoproterozoic tectono-magmatic  
692 activity in lower Belt–Purcell rocks exposed west of Kimberley, British Columbia: Canadian Journal of Earth  
693 Sciences, v. 52, p. 444–465, doi:10.1139/cjes-2014-0215.
- 694 McGlynn, J. C., Hanson, G. N., Irving, E., and Park, J. K., 1974, Paleomagnetism and age of Nonacho Group  
695 sandstones and associated Sparrow dikes, District of Mackenzie: Canadian Journal of Earth Sciences, v. 11, p.  
696 30–42, doi:10.1139/e74-003.
- 697 McLelland, J. M., Selleck, B. W., and Bickford, M., 2010, Review of the Proterozoic evolution of the Grenville  
698 Province, its Adirondack outlier, and the Mesoproterozoic inliers of the Appalachians: From Rodinia to Pangea:  
699 The Lithotectonic Record of the Appalachian Region, p. 21–49, doi:10.1130/2010.1206(02).
- 700 McLelland, J. M., Selleck, B. W., and Bickford, M. E., 2013, Tectonic evolution of the Adirondack Mountains and  
701 Grenville Orogen inliers within the USA: Geoscience Canada, v. 40, p. 318, doi:10.12789/geocanj.2013.40.022.
- 702 McMechan, M. E. and Price, R. A., 1982, Superimposed low-grade metamorphism in the Mount Fisher area,  
703 southeastern British Columbia—implications for the East Kootenay orogeny: Canadian Journal of Earth  
704 Sciences, v. 19, p. 476–489, doi:10.1139/e82-039.
- 705 Meert, J., der Voo, R. V., and Payne, T., 1994, Paleomagnetism of the Catoctin volcanic province: a new  
706 Vendian-Cambrian apparent polar wander path for North America: Journal of Geophysical Research, v. 99, p.  
707 4625–4641.
- 708 Meert, J. G. and Stuckey, W., 2002, Revisiting the paleomagnetism of the 1.476 Ga St. Francois Mountains igneous  
709 province, Missouri: Tectonics, v. 21, doi:10.1029/2000tc001265.
- 710 Meredith, A. S., Collins, A. S., Williams, S. E., Pisarevsky, S., Foden, J. D., Archibald, D. B., Blades, M. L., Alessio,  
711 B. L., Armistead, S., Plavsa, D., and et al., 2017, A full-plate global reconstruction of the Neoproterozoic:  
712 Gondwana Research, v. 50, p. 84–134, doi:10.1016/j.gr.2017.04.001.
- 713 Met Office, 2010 - 2015, Cartopy: a cartographic python library with a matplotlib interface: Exeter, Devon, URL  
714 <http://scitools.org.uk/cartopy>.
- 715 Middleton, R. S., Borradaile, G. J., Baker, D., and Lucas, K., 2004, Proterozoic diabase sills of northern Ontario:  
716 Magnetic properties and history: Journal of Geophysical Research: Solid Earth, v. 109,  
717 doi:10.1029/2003jb002581.

- 718 Mitchell, R. N., Bleeker, W., van Breemen, O., Lecheminant, T. N., Peng, P., Nilsson, M. K. M., and Evans, D.  
719 A. D., 2014, Plate tectonics before 2.0 Ga: Evidence from paleomagnetism of cratons within supercontinent  
720 Nuna: *American Journal of Science*, v. 314, p. 878–894, doi:10.2475/04.2014.03.
- 721 Mitchell, R. N., Hoffman, P. F., and Evans, D. A. D., 2010, Coronation loop resurrected: Oscillatory apparent polar  
722 wander of orosirian (2.05–1.8†ga) paleomagnetic poles from slave craton: *Precambrian Research*, v. 179, p.  
723 121–134.
- 724 Mitchell, R. N., Kilian, T. M., and Evans, D. A. D., 2012, Supercontinent cycles and the calculation of absolute  
725 palaeolongitude in deep time: *Nature*, v. 482, p. 208–211, doi:10.1038/nature10800.
- 726 Müller, R. D., Cannon, J., Qin, X., Watson, R. J., Gurnis, M., Williams, S., Pfaffelmoser, T., Seton, M., Russell, S.  
727 H. J., and Zahirovic, S., 2018, GPlates: Building a virtual earth through deep time: *Geochemistry, Geophysics,  
728 Geosystems*, v. 19, p. 2243–2261, doi:10.1029/2018gc007584.
- 729 Murthy, G., Gower, C., Tubett, M., and Patzold, R., 1992, Paleomagnetism of Eocambrian Long Range dykes and  
730 Double Mer Formation from Labrador, Canada: *Canadian Journal of Earth Sciences*, v. 29, p. 1224–1234,  
731 doi:10.1139/e92-098.
- 732 Murthy, G. S., 1978, Paleomagnetic results from the Nain anorthosite and their tectonic implications: *Canadian  
733 Journal of Earth Sciences*, v. 15, p. 516–525, doi:10.1139/e78-058.
- 734 Nesheim, T. O., Vervoort, J. D., McClelland, W. C., Gilotti, J. A., and Lang, H. M., 2012, Mesoproterozoic  
735 syntectonic garnet within Belt Supergroup metamorphic tectonites: Evidence of Grenville-age metamorphism  
736 and deformation along northwest Laurentia: *Lithos*, v. 134–135, p. 91–107, doi:10.1016/j.lithos.2011.12.008.
- 737 Palin, R. M. and White, R. W., 2015, Emergence of blueschists on Earth linked to secular changes in oceanic crust  
738 composition: *Nature Geoscience*, v. 9, p. 60–64, doi:10.1038/ngeo2605.
- 739 Palmer, H., 1970, Paleomagnetism and correlation of some Middle Keweenawan rocks, Lake Superior: *Canadian  
740 Journal of Earth Science*, v. 7, p. 1410–1436, doi:10.1139/e70-136.
- 741 Palmer, H. C., Merz, B. A., and Hayatsu, A., 1977, The Sudbury dikes of the Grenville Front region:  
742 paleomagnetism, petrochemistry, and K–Ar age studies: *Canadian Journal of Earth Sciences*, v. 14, p. 1867–1887.
- 743 Park, J., Norris, D., and LaRochelle, A., 1989, Paleomagnetism and the origin of the Mackenzie Arc of northwestern  
744 Canada: *Canadian Journal of Earth Science*, v. 26, p. 2194–2203, doi:10.1139/e89-186.
- 745 Park, J. K., Irving, E., and Donaldson, J. A., 1973, Paleomagnetism of the Precambrian Dubawnt Group:  
746 Geological Society of America Bulletin, v. 84, p. 859, doi:10.1130/0016-7606(1973)84<859:potpdg>2.0.co;2.
- 747 Pepresson, S. J., Eglington, B. M., Evans, D. A. D., Huston, D., and Reddy, S. M., 2015, Metallogeny and its link to  
748 orogenic style during the Nuna supercontinent cycle: *Geological Society, London, Special Publications*, v. 424,  
749 doi:10.1144/SP424.5.

- 750 Pérez, F. and Granger, B. E., 2007, IPython: a system for interactive scientific computing: Computing in Science  
751 and Engineering, v. 9, p. 21–29, doi:10.1109/MCSE.2007.53.
- 752 Pesonen, L., 1979, Paleomagnetism of late Precambrian Keweenawan igneous and baked contact rocks from  
753 Thunder Bay district, northern Lake Superior: Bulletin of the Geological Society of Finland, v. 51, p. 27–44.
- 754 Pesonen, L. J. and Halls, H., 1979, The paleomagnetism of Keweenawan dikes from Baraga and Marquette  
755 Counties, northern Michigan: Canadian Journal of Earth Science, v. 16, p. 2136–2149, doi:10.1139/e79-201.
- 756 Piispa, E. J., Smirnov, A. V., Pesonen, L. J., and Mitchell, R. H., 2018, Paleomagnetism and geochemistry of  
757 1144-ma lamprophyre dikes, Northwestern Ontario: Implications for the North American polar wander and plate  
758 velocities: Journal of Geophysical Research: Solid Earth, doi:10.1029/2018jb015992.
- 759 Piper, J., 1992, The palaeomagnetism of major (Middle Proterozoic) igneous complexes, South Greenland and the  
760 Gardar apparent polar wander track: Precambrian Research, v. 54, p. 153 – 172,  
761 doi:10.1016/0301-9268(92)90068-Y.
- 762 Piper, J. and Stearn, J., 1977, Palaeomagnetism of the dyke swarms of the Gardar Igneous Province, south  
763 Greenland: Physics of the Earth and Planetary Interiors, v. 14, p. 345–358, doi:10.1016/0031-9201(77)90167-4.
- 764 Piper, J. D. A., 1977, Palaeomagnetism of the giant dykes of Tugtutoq and Narssaq Gabbro, Gardar Igneous  
765 Province, South Greenland: Bull. Geol. Soc. Den, v. 26, p. 85–94.
- 766 Pisarevsky, S. A., Elming, S.-Å., Pesonen, L. J., and Li, Z.-X., 2014, Mesoproterozoic paleogeography:  
767 Supercontinent and beyond: Precambrian Research, v. 244, p. 207–225, doi:10.1016/j.precamres.2013.05.014.
- 768 Pullaiah, G. and Irving, E., 1975, Paleomagnetism of the contact aureole and late dikes of the Otto stock, Ontario,  
769 and its application to early proterozoic apparent polar wandering: Canadian Journal of Earth Sciences, v. 12, p.  
770 1609–1618, doi:10.1139/e75-143.
- 771 Rapalini, A. E., 2018, The assembly of western Gondwana: Reconstruction based on paleomagnetic data: Geology  
772 of Southwest Gondwana, p. 3–18, doi:10.1007/978-3-319-68920-3\_1.
- 773 Redden, J., Peterman, Z., Zartman, R., and De-Witt, E., 1990, U-Th-Pb geochronology and preliminary  
774 interpretation of Precambrian tectonic events in the Black Hills, South Dakota: *In* The Early Proterozoic  
775 Trans-Hudson Orogen, Geological Association of Canada Special Paper 37, p. 229–251.
- 776 Rivers, T., 2008, Assembly and preservation of lower, mid, and upper orogenic crust in the Grenville  
777 Province—implications for the evolution of large hot long-duration orogens: Precambrian Research, v. 167, p.  
778 237–259, doi:10.1016/j.precamres.2008.08.005.
- 779 Robert, B., Besse, J., Blein, O., Greff-Lefftz, M., Baudin, T., Lopes, F., Meslouh, S., and Belbadaoui, M., 2017,  
780 Constraints on the ediacaran inertial interchange true polar wander hypothesis: A new paleomagnetic study in  
781 morocco (west african craton): Precambrian Research, v. 295, p. 90–116, doi:10.1016/j.precamres.2017.04.010.

- 782 Robertson, W. and Fahrig, W., 1971, The great Logan Loop - the polar wandering path from Canadian shield rocks  
783 during the Neohelikian era: *Canadian Journal of Earth Science*, v. 8, p. 1355–1372, doi:10.1139/e71-125.
- 784 Roest, W. R. and Srivastava, S. P., 1989, Sea-floor spreading in the labrador sea: A new reconstruction: *Geology*,  
785 v. 17, p. 1000, doi:10.1130/0091-7613(1989)017<1000:sfsitl>2.3.co;2.
- 786 Rooney, A. D., Austermann, J., Smith, E. F., Li, Y., Selby, D., Dehler, C. M., Schmitz, M. D., Karlstrom, K. E.,  
787 and Macdonald, F. A., 2017, Coupled Re-Os and U-Pb geochronology of the Tonian Chuar Group, Grand  
788 Canyon: *GSA Bulletin*, doi:10.1130/b31768.1.
- 789 Ross, G. M., 1991, Tectonic setting of the Windermere Supergroup revisited: *Geology*, v. 19, p. 1125,  
790 doi:10.1130/0091-7613(1991)019<1125:tsotws>2.3.co;2.
- 791 Schmidt, P. W., 1980, Paleomagnetism of igneous rocks from the Belcher Islands, Northwest Territories, Canada:  
792 *Canadian Journal of Earth Sciences*, v. 17, p. 807–822, doi:10.1139/e80-081.
- 793 Schulz, K. J. and Cannon, W. F., 2007, The Penokean orogeny in the Lake Superior region: *Precambrian Research*,  
794 v. 157, p. 4–25, doi:10.1016/j.precamres.2007.02.022.
- 795 Schwarz, E. J., Clark, K. R., and Fujiwara, Y., 1982, Paleomagnetism of the Sutton Lake Proterozoic inlier,  
796 Ontario, Canada: *Canadian Journal of Earth Sciences*, v. 19, p. 1330–1332, doi:10.1139/e82-114.
- 797 Selkin, P. A., Gee, J. S., Meurer, W. P., and Hemming, S. R., 2008, Paleointensity record from the 2.7 Ga Stillwater  
798 Complex, Montana: *Geochem. Geophys. Geosyst.*, v. 9, p. 10.1029/2008GC001,950.
- 799 Skipton, D. R., St-Onge, M. R., Schneider, D. A., and McFarlane, C. R. M., 2016, Tectonothermal evolution of the  
800 middle crust in the Trans-Hudson Orogen, Baffin Island, Canada: Evidence from petrology and monazite  
801 geochronology of sillimanite-bearing migmatites: *Journal of Petrology*, v. 57, p. 1437–1462,  
802 doi:10.1093/petrology/egw046.
- 803 Slagstad, T., Culshaw, N. G., Daly, J. S., and Jamieson, R. A., 2009, Western Grenville Province holds key to  
804 midcontinental Granite-Rhyolite Province enigma: *Terra Nova*, v. 21, p. 181–187,  
805 doi:10.1111/j.1365-3121.2009.00871.x.
- 806 St-Onge, M. R., Van Gool, J. A. M., Garde, A. A., and Scott, D. J., 2009, Correlation of Archaean and  
807 Palaeoproterozoic units between northeastern Canada and western Greenland: constraining the pre-collisional  
808 upper plate accretionary history of the Trans-Hudson orogen: *Geological Society, London, Special Publications*,  
809 v. 318, p. 193–235, doi:10.1144/sp318.7.
- 810 Stern, R. J. and Miller, N. R., 2018, Did the transition to plate tectonics cause neoproterozoic snowball earth?:  
811 *Terra Nova*, v. 30, p. 87–94, doi:10.1111/ter.12321.

- 812 Stern, R. J., Tsujimori, T., Harlow, G., and Groat, L. A., 2013, Plate tectonic gemstones: Geology, v. 41, p.  
813 723–726, doi:10.1130/g34204.1.
- 814 Swanson-Hysell, N. L., Burgess, S. D., Maloof, A. C., and Bowring, S. A., 2014a, Magmatic activity and plate  
815 motion during the latent stage of Midcontinent Rift development: Geology, v. 42, p. 475–478,  
816 doi:10.1130/G35271.1.
- 817 Swanson-Hysell, N. L., Ramezani, J., Fairchild, L. M., and Rose, I. R., 2019, Failed rifting and fast drifting:  
818 Midcontinent Rift development, Laurentia’s rapid motion and the driver of Grenvillian orogenesis: GSA Bulletin,  
819 doi:10.1130/b31944.1.
- 820 Swanson-Hysell, N. L., Vaughan, A. A., Mustain, M. R., and Asp, K. E., 2014b, Confirmation of progressive plate  
821 motion during the Midcontinent Rift’s early magmatic stage from the Osler Volcanic Group, Ontario, Canada:  
822 Geochemistry Geophysics Geosystems, v. 15, p. 2039–2047, doi:10.1002/2013GC005180.
- 823 Symons, D. and Chiasson, A., 1991, Paleomagnetism of the Callander Complex and the Cambrian apparent polar  
824 wander path for North America: Canadian Journal of Earth Science, v. 1991, p. 355–363, doi:10.1139/e91-032.
- 825 Symons, D., Symons, T., and Lewchuk, M., 2000, Paleomagnetism of the Deschambault pegmatites: Stillstand and  
826 hairpin at the end of the Paleoproterozoic Trans-Hudson Orogeny, Canada: Physics and Chemistry of the Earth,  
827 Part A: Solid Earth and Geodesy, v. 25, p. 479–487, doi:10.1016/s1464-1895(00)00074-0.
- 828 Symons, D. T. A. and Mackay, C. D., 1999, Paleomagnetism of the Boot-Phantom pluton and the amalgamation of  
829 the juvenile domains in the Paleoproterozoic Trans-Hudson Orogen, Canada: In Sinha, A. K., ed., Basement  
830 Tectonics 13, Springer Netherlands, Dordrecht, p. 313–331, doi:10.1007/978-94-011-4800-9\\_\\_18.
- 831 Tanczyk, E., Lapointe, P., Morris, W., and Schmidt, P., 1987, A paleomagnetic study of the layered mafic intrusions  
832 at Sept-Iles, Quebec: Canadian Journal of Earth Science, v. 24, p. 1431–1438, doi:10.1139/e87-135.
- 833 Tauxe, L. and Kodama, K., 2009, Paleosecular variation models for ancient times: Clues from Keweenawan lava  
834 flows: Physics of the Earth and Planetary Interiors, v. 177, p. 31–45, doi:10.1016/j.pepi.2009.07.006.
- 835 Tauxe, L., Shaar, R., Jonestrask, L., Swanson-Hysell, N., Minnett, R., Koppers, A., Constable, C., Jarboe, N.,  
836 Gaastra, K., and Fairchild, L., 2016, PmagPy: Software package for paleomagnetic data analysis and a bridge to  
837 the Magnetics Information Consortium (MagIC) Database: Geochemistry, Geophysics, Geosystems,  
838 doi:10.1002/2016GC006307.
- 839 Torsvik, T. H. and Cocks, L. R. M., 2017, Earth history and palaeogeography: Cambridge University Press,  
840 doi:10.1017/9781316225523.
- 841 Torsvik, T. H., van der Voo, R., Doubrovine, P. V., Burke, K., Steinberger, B., Ashwal, L. D., Trønnes, R. G.,  
842 Webb, S. J., and Bull, A. L., 2014, Deep mantle structure as a reference frame for movements in and on the  
843 Earth: Proceedings of the National Academy of Sciences, doi:10.1073/pnas.1318135111.

- 844 Torsvik, T. H., Van der Voo, R., Preeden, U., Mac Niocaill, C., Steinberger, B., Doubrovine, P. V., van Hinsbergen,  
 845 D. J. J., Domeier, M., Gaina, C., Tohver, E., Meert, J. G., McCausland, P. J. A., and Cocks, L. R. M., 2012,  
 846 Phanerozoic polar wander, palaeogeography and dynamics: *Earth-Science Reviews*, v. 114, p. 325–368,  
 847 doi:10.1016/j.earscirev.2012.06.007.
- 848 Veikkolainen, T., Pesonen, L., and Evans, D. D., 2014, PALEOMAGIA: A PHP/MYSQL database of the  
 849 Precambrian paleomagnetic data: p. 1–17, doi:10.1007/s11200-013-0382-0.
- 850 Warnock, A., Kodama, K., and Zeitler, P., 2000, Using thermochronometry and low-temperature demagnetization  
 851 to accurately date Precambrian paleomagnetic poles: *Journal of Geophysical Research*, v. 105, p. 19,435–19,453,  
 852 doi:10.1029/2000jb900114.
- 853 Weil, A., Geissman, J., Heizler, M., and Van der Voo, R., 2003, Paleomagnetism of Middle Proterozoic mafic  
 854 intrusions and Upper Proterozoic (Nankoweap) red beds from the Lower Grand Canyon Supergroup, Arizona:  
 855 *Tectonophysics*, v. 375, p. 199–220, doi:10.1016/S0040-1951(03)00339-1.
- 856 Weil, A. B., Geissman, J. W., and Ashby, J. M., 2006, A new paleomagnetic pole for the Neoproterozoic Uinta  
 857 Mountain supergroup, Central Rocky Mountain States, USA: *Precambrian Research*, v. 147, p. 234–259,  
 858 doi:10.1016/j.precamres.2006.01.017.
- 859 Weller, O. M. and St-Onge, M. R., 2017, Record of modern-style plate tectonics in the Palaeoproterozoic  
 860 Trans-Hudson orogen: *Nature Geoscience*, v. 10, doi:10.1038/ngeo2904.
- 861 Whitmeyer, S. and Karlstrom, K., 2007, Tectonic model for the Proterozoic growth of North America: *Geosphere*,  
 862 v. 3, p. 220–259, doi:10.1130/GES00055.1.
- 863 Witkosky, R. and Wernicke, B. P., 2018, Subsidence history of the Ediacaran Johnnie Formation and related strata  
 864 of southwest Laurentia: Implications for the age and duration of the Shuram isotopic excursion and animal  
 865 evolution: *Geosphere*, v. 14, p. 2245–2276, doi:10.1130/ges01678.1.
- 866 Zhang, S., Li, Z.-X., Evans, D. A. D., Wu, H., Li, H., and Dong, J., 2012, Pre-Rodinia supercontinent Nuna shaping  
 867 up: A global synthesis with new paleomagnetic results from North China: *Earth and Planetary Science Letters*,  
 868 v. 353–354, p. 145–155.

**Table 1.** Rotations of separated terranes

Block	Euler pole longitude	Euler pole latitude	rotation angle	note and citation
Greenland	-118.5	67.5	-13.8	Cenozoic separation of Greenland from Laurentia associated with opening of Baffin Bay and the Labrador Sea (Roest and Srivastava, 1989)
Scotland	161.9	78.6	-31.0	Reconstructing Atlantic opening following Torsvik and Cocks (2017)
Svalbard	125.0	-81.0	68	Rotate Svalbard to Laurentia in fit that works well with East Greenland basin according to Maloof et al. (2006)

terrane	unit name	rating	site lon	site lat	plon	plat	$A_{95}$	age	pole reference
Laurentia-Wyoming	Stillwater Complex - C2	A	249.2	45.2	335.8	-83.6	4.0	$2705^{+4}_{-4}$	Selkin et al. (2008)
Laurentia-Superior(East)	Otto Stock dykes and aureole	B	279.9	48.0	227.0	69.0	4.8	$2676^{+5}_{-5}$	Pullaiah and Irving (1975)
Laurentia-Slave	Defeat Suite	B	245.5	62.5	64.0	-1.0	15.0	$2625^{+5}_{-5}$	Mitchell et al. (2014)
Laurentia-Superior(East)	Ptarmigan-Mistassini dykes	B	287.0	54.0	213.0	-45.3	13.8	$2505^{+2}_{-2}$	Evans and Halls (2010)
Laurentia-Superior(East)	Matachewan dykes	A	278.0	48.0	238.3	-44.1	1.6	$2466^{+23}_{-23}$	Evans and Halls (2010)
Laurentia-Superior(East)	R	A	278.0	48.0	239.5	-52.3	2.4	$2446^{+3}_{-3}$	Evans and Halls (2010)
Laurentia-Slave	Malley dykes	A	249.8	64.2	310.0	-50.8	6.7	$2231^{+2}_{-2}$	Buchan et al. (2012)
Laurentia-Superior(East)	Senneterre dykes	A	283.0	49.0	284.3	-15.3	5.5	$2218^{+6}_{-6}$	Buchan et al. (1993)
Laurentia-Superior(East)	Nipissing N1 sills	A	279.0	47.0	272.0	-17.0	10.0	$2217^{+4}_{-4}$	Buchan et al. (2000)
Laurentia-Slave	Dogrib dykes	A	245.5	62.5	315.0	-31.0	7.0	$2193^{+2}_{-2}$	Mitchell et al. (2014)
Laurentia-Superior(East)	Biscotasing dykes	A	280.0	48.0	223.9	26.0	7.0	$2170^{+3}_{-3}$	Evans and Halls (2010)
Laurentia-Wyoming	Rabbit Creek, Powder River and South Path Dykes	A	252.8	43.9	339.2	65.5	7.6	$2160^{+11}_{-8}$	Kilian et al. (2015)
Laurentia-Slave	Indin dykes	A	245.6	62.5	256.0	-36.0	7.0	$2126^{+3}_{-18}$	Buchan et al. (2016)
Laurentia-Superior(West)	Marathon dykes N	A	275.0	49.0	198.2	45.4	7.7	$2124^{+3}_{-3}$	Halls et al. (2008)

Continued on next page

terrane	unit name	rating	site lon	site lat	plon	plat	$A_{95}$	age	pole reference
Laurentia-Superior(West)	Marathon dykes R	A	275.0	49.0	182.2	55.1	7.5	$2104^{+3}_{-3}$	Halls et al. (2008)
Laurentia-Superior(West)	Cauchon Lake dykes	A	263.0	56.0	180.9	53.8	7.7	$2091^{+2}_{-2}$	Evans and Halls (2010)
Laurentia-Superior(West)	Fort Frances dykes	A	266.0	48.0	184.6	42.8	6.1	$2077^{+5}_{-5}$	Evans and Halls (2010)
Laurentia-Superior(East)	Lac Esprit dykes	A	282.0	53.0	170.5	62.0	6.4	$2069^{+1}_{-1}$	Evans and Halls (2010)
Laurentia-Greenland-Nain	Kangamiut Dykes	B	307.0	66.0	273.8	17.1	2.7	$2042^{+12}_{-12}$	Fahrig and Bridgwater (1976)
Laurentia-Slave	Lac de Gras dykes	A	249.6	64.4	267.9	11.8	7.1	$2026^{+5}_{-5}$	Buchan et al. (2009)
Laurentia-Superior(East)	Minto dykes	A	285.0	57.0	171.5	38.7	13.1	$1998^{+2}_{-2}$	Evans and Halls (2010)
Laurentia-Slave	Rifle Formation	B	252.9	65.9	341.0	14.0	7.7	$1963^{+6}_{-6}$	Evans and Hoye (1981)
Laurentia-Rae	Clearwater Anorthosite	B	251.6	57.1	311.8	6.5	2.9	$1917^{+7}_{-7}$	Halls and Hanes (1999)
Laurentia-Wyoming	Sourdough mafic dike swarm	A	-108.3	44.7	292.0	49.2	8.1	$1899^{+5}_{-5}$	Kilian et al. (2016)
Laurentia-Slave	Ghost Dike Swarm	A	244.6	62.6	286.0	-2.0	6.0	$1887^{+5}_{-9}$	Buchan et al. (2016)
Laurentia-Slave	Mean Se-ton/Akaitcho/Mara	B	250.0	65.0	260.0	-6.0	4.0	$1885^{+5}_{-5}$	Mitchell et al. (2010)
Laurentia-Slave	Mean Kahochella, Peacock Hills	B	250.0	65.0	285.0	-12.0	7.0	$1882^{+4}_{-4}$	Mitchell et al. (2010)
Laurentia-Superior(West)	Molson (B+C2) dykes	A	262.0	55.0	218.0	28.9	3.8	$1879^{+6}_{-6}$	Evans and Halls (2010)

Continued on next page

terrane	unit name	rating	site lon	site lat	plon	plat	$A_{95}$	age	pole reference
Laurentia-Slave	Douglas Peninsula Formation, Pethei Group	B	249.7	62.8	258.0	-18.0	14.2	$1876^{+10}_{-10}$	Irving and McGlynn (1979)
Laurentia-Slave	Takiyuak Formation	B	246.9	66.1	249.0	-13.0	8.0	$1876^{+10}_{-10}$	Irving and McGlynn (1979)
Laurentia-Superior	Haig/Flaherty/Sutton Mean	B	279.0	56.0	245.8	1.0	3.9	$1870^{+1}_{-1}$	Nordic workshop calculation based on data of Schmidt (1980); Schwarz et al. (1982)
Laurentia-Slave	Pearson A/Peninsular/Kilohigok sills	A	250.0	65.0	269.0	-22.0	6.0	$1870^{+4}_{-4}$	Mitchell et al. (2010)
Laurentia-Trans-Hudson orogen	Boot-Phantom Pluton	B	258.1	54.7	275.4	62.4	7.9	$1838^{+1}_{-1}$	Symons and Mackay (1999)
Laurentia-Rae	Sparrow Dykes	B	250.2	61.6	291.0	12.0	7.9	$1827^{+4}_{-4}$	McGlynn et al. (1974)
Laurentia-Rae	Martin Formation	A	251.4	59.6	288.0	-9.0	8.5	$1818^{+4}_{-4}$	Evans and Bingham (1973)
Laurentia	Dubawnt Group	B	265.6	64.1	277.0	7.0	8.0	$1785^{+35}_{-35}$	Park et al. (1973)
Laurentia-Trans-Hudson orogen	Deschambault Pegmatites	B	256.7	54.9	276.0	67.5	7.7	$1766^{+5}_{-5}$	Symons et al. (2000)
Laurentia-Trans-Hudson orogen	Jan Lake Granite	B	257.2	54.9	264.3	24.3	16.9	$1758^{+1}_{-1}$	Gala et al. (1995)
Laurentia	Cleaver Dykes	A	242.0	67.5	276.7	19.4	6.1	$1741^{+5}_{-5}$	Irving (2004)
Laurentia-Greenland	Melville Bugt dia-base dykes	B	303.0	74.6	273.8	5.0	8.7	$1633^{+5}_{-5}$	Halls et al. (2011)
Laurentia	Western Channel Diabase	A	242.2	66.4	245.0	9.0	6.6	$1590^{+3}_{-3}$	Irving and Park (1972)

Continued on next page

terrane	unit name	rating	site lon	site lat	plon	plat	A <sub>95</sub>	age	pole reference
Laurentia	St.Francois Mountains Acidic Rocks	A	269.5	37.5	219.0	-13.2	6.1	1476 <sup>+16</sup> <sub>-16</sub>	Meert and Stuckey (2002)
Laurentia	Michikamau Intrusion	A	296.0	54.5	217.5	-1.5	4.7	1460 <sup>+5</sup> <sub>-5</sub>	Emslie et al. (1976)
Laurentia	Spokane Formation	A	246.8	48.2	215.5	-24.8	4.7	1458 <sup>+13</sup> <sub>-13</sub>	Elston et al. (2002)
Laurentia	Snowslip Formation	A	245.9	47.9	210.2	-24.9	3.5	1450 <sup>+14</sup> <sub>-14</sub>	Elston et al. (2002)
Laurentia	Tobacco Root dykes	B	247.6	47.4	216.1	8.7	10.5	1448 <sup>+49</sup> <sub>-49</sub>	Harlan et al. (2008)
Laurentia	Purcell Lava	A	245.1	49.4	215.6	-23.6	4.8	1443 <sup>+7</sup> <sub>-7</sub>	Elston et al. (2002)
Laurentia	Rocky Mountain intrusions	B	253.8	40.3	217.4	-11.9	9.7	1430 <sup>+15</sup> <sub>-15</sub>	Nordic workshop calculation based on data of Harlan et al. (1994); Harlan and Geissman (1998)
Laurentia	Mistastin Pluton	B	296.3	55.6	201.5	-1.0	7.6	1425 <sup>+25</sup> <sub>-25</sub>	Fahrig and Jones (1976)
Laurentia	McNamara Formation	A	246.4	46.9	208.3	-13.5	6.7	1401 <sup>+6</sup> <sub>-6</sub>	Elston et al. (2002)
Laurentia	Pilcher, Garnet Range and Libby Formations	A	246.4	46.7	215.3	-19.2	7.7	1385 <sup>+23</sup> <sub>-23</sub>	Elston et al. (2002)
Laurentia-Greenland	Zig-Zag Dal Basalts	B	334.8	81.2	242.8	12.0	3.8	1382 <sup>+2</sup> <sub>-2</sub>	Marcussen and Abrahamsen (1983)
Laurentia-Greenland	Midsommersoe Dolerite	B	333.4	81.6	242.0	6.9	5.1	1382 <sup>+2</sup> <sub>-2</sub>	Marcussen and Abrahamsen (1983)
Laurentia-Greenland	Victoria Fjord dolerite dykes	B	315.3	81.5	231.7	10.3	4.3	1382 <sup>+2</sup> <sub>-2</sub>	Abrahamsen and Van Der Voo (1987)

Continued on next page

terrane	unit name	rating	site lon	site lat	plon	plat	$A_{95}$	age	pole reference
Laurentia	Nain Anorthosite	B	298.2	56.5	206.7	11.7	2.2	$1305^{+15}_{-15}$	Murthy (1978)
Laurentia-Greenland	North Qoroq intrusives	B	314.6	61.1	202.6	13.2	8.3	$1275^{+1}_{-1}$	Piper (1992)
Laurentia-Greenland	Kungnat Ring Dyke	B	311.7	61.2	198.7	3.4	3.2	$1275^{+2}_{-2}$	Piper and Stearn (1977)
Laurentia	Mackenzie dykes	A	250.0	65.0	190.0	4.0	5.0	$1267^{+2}_{-2}$	Buchan et al. (2000)
	grand mean								
Laurentia-Greenland	West Gardar Dolerite Dykes	B	311.7	61.2	201.7	8.7	6.6	$1244^{+8}_{-8}$	Piper and Stearn (1977)
Laurentia-Greenland	West Gardar Lamprophyre Dykes	B	311.7	61.2	206.4	3.2	7.2	$1238^{+11}_{-11}$	Piper and Stearn (1977)
Laurentia	Sudbury Dykes	A	278.6	46.3	192.8	-2.5	2.5	$1237^{+5}_{-5}$	Palmer et al. (1977)
	Combined								
Laurentia-Scotland	Stoer Group	B	354.5	58.0	238.4	37.2	7.7	$1199^{+70}_{-70}$	Nordic workshop calculation
Laurentia-Greenland	Narssaq Gabbro	B	313.8	60.9	225.4	31.6	9.7	$1184^{+5}_{-5}$	Piper (1977)
Laurentia-Greenland	Hviddal Giant Dyke	B	313.7	60.9	215.3	33.2	9.6	$1184^{+5}_{-5}$	Piper (1977)
Laurentia-Greenland	South Qoroq Intr.	A	314.6	61.1	215.9	41.8	13.1	$1163^{+2}_{-2}$	Piper (1992)
Laurentia-Greenland	Giant Gabbro Dykes	B	313.7	60.9	226.1	42.3	9.4	$1163^{+2}_{-2}$	Piper (1977)
Laurentia-Greenland	NE-SW Trending dykes	B	314.6	61.1	230.8	33.4	5.7	$1160^{+5}_{-5}$	Piper (1992)
Laurentia	Ontario lamprophyre dykes	A	273.3	48.8	223.3	58.0	9.2	$1143^{+10}_{-10}$	Piispa et al. (2018)

Continued on next page

terrane	unit name	rating	site lon	site lat	plon	plat	$A_{95}$	age	pole reference
Laurentia	Abitibi Dykes	A	279.0	48.0	215.5	48.8	14.1	$1141^{+2}_{-2}$	Ernst and Buchan (1993)
Laurentia	Nipigon sills and lavas	A	270.9	49.1	217.8	47.2	4.0	$1109^{+2}_{-2}$	Nordic workshop calculation based on data of Palmer (1970); Robertson and Fahrig (1971); Pesonen (1979); Pesonen and Halls (1979); Middleton et al. (2004); Borradaile and Middleton (2006)
Laurentia	Lowermost Mamainse Point volcanics -R1	A	275.3	47.1	227.0	49.5	5.3	$1109^{+2}_{-3}$	Swanson-Hysell et al. (2014a)
Laurentia	Lower Osler volcanics -R	A	272.3	48.8	218.6	40.9	4.8	$1108^{+3}_{-3}$	Swanson-Hysell et al. (2014b)
Laurentia	Middle Osler volcanics -R	A	272.4	48.8	211.3	42.7	8.2	$1107^{+4}_{-4}$	Swanson-Hysell et al. (2014b)
Laurentia	Upper Osler volcanics -R	A	272.4	48.7	203.4	42.3	3.7	$1105^{+1}_{-1}$	Halls (1974); Swanson-Hysell et al. (2014b, 2019)
Laurentia	Lower Mamainse Point volcanics -R2	A	275.3	47.1	205.2	37.5	4.5	$1105^{+3}_{-4}$	Swanson-Hysell et al. (2014a)
Laurentia	Mamainse Point volcanics -C (lower N, upper R)	A	275.3	47.1	189.7	36.1	4.9	$1101^{+1}_{-1}$	Swanson-Hysell et al. (2014a)
Laurentia	North Shore lavas -N	A	268.7	46.3	181.7	31.1	2.1	$1097^{+3}_{-3}$	Tauxe and Kodama (2009); Swanson-Hysell et al. (2019)

Continued on next page

terrane	unit name	rating	site lon	site lat	plon	plat	$A_{95}$	age	pole reference
Laurentia	Portage Lake Volcanics	A	271.2	47.0	182.5	27.5	2.3	$1095^{+3}_{-3}$	Books (1972); Hnat et al. (2006) as calculated in Swanson-Hysell et al. (2019)
Laurentia	Chengwatana Volcanics	B	267.3	45.4	186.1	30.9	8.2	$1095^{+2}_{-2}$	Kean et al. (1997)
Laurentia	Uppermost Mainse Point volcanics -N	A	275.3	47.1	183.2	31.2	2.5	$1094^{+6}_{-4}$	Swanson-Hysell et al. (2014a)
Laurentia	Cardenas Basalts and Intrusions	B	248.1	36.1	185.0	32.0	8.0	$1091^{+5}_{-5}$	Weil et al. (2003)
Laurentia	Schroeder Lutsen Basalts	A	269.1	47.5	187.8	27.1	3.0	$1090^{+2}_{-7}$	Fairchild et al. (2017)
Laurentia	Central Arizona diabases -N	A	249.2	33.7	175.3	15.7	7.0	$1088^{+11}_{-11}$	Donadini et al. (2011)
Laurentia	Lake Shore Traps	A	271.9	47.6	186.4	23.1	4.0	$1086^{+1}_{-1}$	Kulakov et al. (2013)
Laurentia	Michipicoten Island Formation	A	274.3	47.7	174.7	17.0	4.4	$1084^{+1}_{-1}$	Fairchild et al. (2017)
Laurentia	Nonesuch Shale	B	271.5	47.0	178.1	7.6	5.5	$1080^{+4}_{-10}$	Henry et al. (1977)
Laurentia	Freda Sandstone	B	271.5	47.0	179.0	2.2	4.2	$1070^{+14}_{-10}$	Henry et al. (1977)
Laurentia	Haliburton Intrusions	B	281.4	45.0	141.9	-32.6	6.3	$1015^{+15}_{-15}$	Warnock et al. (2000)
Laurentia-Scotland	Torridon Group	B	354.3	57.9	220.9	-17.7	7.1	$925^{+145}_{-145}$	Nordic workshop calculation
Laurentia-Svalbard	Lower Grusdievbreen Formation	B	18.0	79.0	204.9	19.6	10.9	$831^{+20}_{-20}$	Maloof et al. (2006)

Continued on next page

terrane	unit name	rating	site lon	site lat	plon	plat	A <sub>95</sub>	age	pole reference
Laurentia-Svalbard	Upper Grus-dievbreen Formation	B	18.2	78.9	252.6	-1.1	6.2	800 <sup>+11</sup> <sub>-11</sub>	Maloof et al. (2006)
Laurentia	Gunbarrel dykes	B	248.7	44.8	129.4	13.9	8.2	778 <sup>+2</sup> <sub>-2</sub>	Nordic workshop calculation based on data of Harlan (1993); Harlan et al. (1997)
Laurentia	Tsezotene Sills	B	235.0	63.5	137.8	1.6	5.0	778 <sup>+2</sup> <sub>-2</sub>	Park et al. (1989)
Laurentia	Uinta Mountain Group	B	250.7	40.8	161.3	0.8	4.7	775 <sup>+25</sup> <sub>-25</sub>	Weil et al. (2006)
Laurentia-Svalbard	Svanbergfjellet Formation	B	18.0	78.5	226.8	25.9	5.8	760 <sup>+30</sup> <sub>-30</sub>	Maloof et al. (2006)
Laurentia	Franklin event grand mean	A	275.4	73.0	162.1	6.7	3.0	724 <sup>+3</sup> <sub>-3</sub>	Denyszyn et al. (2009a)
Laurentia	Long Range Dykes	B	303.3	53.7	355.3	19.0	17.4	615 <sup>+2</sup> <sub>-2</sub>	Murthy et al. (1992)
Laurentia	Baie des Moutons complex	B	301.0	50.8	321.5	-34.2	15.4	583 <sup>+2</sup> <sub>-2</sub>	McCausland et al. (2011)
Laurentia	Baie des Moutons complex	B	301.0	50.8	332.7	42.6	12.0	583 <sup>+2</sup> <sub>-2</sub>	McCausland et al. (2011)
Laurentia	Callander Alkaline Complex	B	280.6	46.2	301.4	46.3	6.0	575 <sup>+5</sup> <sub>-5</sub>	Symons and Chiasson (1991)
Laurentia	Catoctin Basalts	B	281.8	38.5	296.7	42.0	17.5	572 <sup>+5</sup> <sub>-5</sub>	Meert et al. (1994)
Laurentia	Sept-Iles layered intrusion	B	293.5	50.2	321.0	-20.0	6.7	565 <sup>+4</sup> <sub>-4</sub>	Tanczyk et al. (1987)